Revista Española de Micropaleontología, 42 (3), 2010, pp. 321-344

ISSN: 0556-655X

Nannoplankton and planktonic foraminifera biostratigraphy of the eastern Betics during the Tortonian (SE Spain)

Carlos Lancis[1], José Enrique Tent-Manclús[1], Jesús Miguel Soria[1], Hugo Corbí[1], Jaume Dinarès-Turell[2] and Alfonso Yébenes[1]

[1] Universidad de Alicante, Departamento de Ciencias de la Tierra y del Medio Ambiente. Aptdo. 99. 03080 San Vicente del Raspeig, Alicante. Carlos.lancis@ua.es
[2] Istituto Nazionale di Geofisica e Vulcanologia, Via di Vigna Murata, 605, 00143 Roma, Italy.

Resumen

El final del Serravalliense y principio del Tortoniense es un periodo de fuerte actividad tectónica en la Cordillera Bética. Además, existe un debate sobre la existencia de sedimentos de edad Tortoniense inferior al no existir claras atribuciones fósiles en esa edad. Estos sedimentos se asignan a dicha edad por criterios indirectos, tanto estratigráficos como por la ausencia de contenido fósil más antiguo o más reciente. En este trabajo se describe la sección compuesta de *Les Moreres-Albatera*, que es probablemente una de las secciones más completas de edad Tortoniense en la bibliografía de la Cordillera Bética, pese a tener un importante hiato de cerca de 1 Millón de años ligado a un evento tectónico intra-Tortoniense. La sección presenta dos unidades litológicas calizas a la base (El Castellà) y al techo (Las Ventanas) y dos unidades intermedias margosas, la inferior, llamada Les Moreres, y la superior, Galería de los Suizos se encuentran separadas por el conglomerado de la Raya del Búho. Se han identificado las biozonas de nanofósiles calcáreos CN5b/NN7 a CN9a/NN11a (Okada & Bukry, 1980; Martini, 1971) y de foraminíferos planctónicos de MMi9 a MMi12a (Lourens *et al.*, 2004). La biostratigrafía de los primeros ha permitido identificar un hiato que incluye la parte alta de las biozonas CN7/NN9 hasta la parte baja de CN9a/NN11a (Okada & Bukry, 1980; Martini, 1971). La integración de los datos biostratigráficos con los paleomagnéticos en la sección *Albatera* permite la calibración del límite de los magnetocrones C4r.1r/C4n.2n.

Palabras clave: Cordillera Bética, Mioceno, Tortoniense, Nanoplancton calcáreo, Foraminíferos planctónicos, Bioestratigrafía.

Abstract

The Serravallian-Tortonian boundary was a time of strong tectonic activity in the Betic Cordillera. The Early Tortonian sediments continue to be under debate because no clear fossil attributions are available. These sediments have been assigned an Early Tortonian age by indirect stratigraphic criteria or by the absence of fossil content older or younger in age. The present work documents the *Les Moreres-Albatera* composite section, probably the most complete section of the Tortonian age in the Betic Cordillera, despite a major time gap of about 1 Ma due to an intra-Tortonian tectonic event. The section has two limestone units at the bottom (El Castellà) and the top (Las Ventanas) and two intermediate marly units, the lower Les Moreres and the upper Galería de los Suizos divided by the Raya del Búho Conglomerate. The calcareous nannoplankton biozones from CN5b/NN7 to CN9a/NN11a (Okada & Bukry, 1980; Martini, 1971) have been identified, as have the planktonic foraminifera biozones from MMi9 to MMi12a (Lourens *et al.* 2004). The calcareous nannoplankton biostratigraphy has allowed the identification of a time gap that includes the upper part of the CN7/NN9 biozones to the lower part of the CN9a/NN11a (Okada &Bukry, 1980; Martini, 1971). The integrated palaeomagnetic and biostratigraphic study of *Albatera* section has allowed to calibrate the C4r.1r/C4n.2n chron boundary.

Key words: Betic Cordillera, Miocene, Tortonian, Calcareous nannoplankton, Planktonic foraminifera, Biostratigraphy.

1. INTRODUCTION

The convergence of Europe and Africa during the Cretaceous-Tertiary resulted in the narrowing and partial closure of the Atlantic-Mediterranean passages, and the building up of the Betic and Rif cordilleras to form an arc-shaped mountain belt lying at both sides of the Strait of Gibraltar (Fig. 1).

The Miocene is a crucial period for understanding the geodynamic evolution of the Betic Cordillera within the Western Mediterranean orogenic system. Those major orogenic events that shaped the Betic-Rif orogen occurred during the Early and Middle Miocene (Vera, 2004). A process of lithospheric reorganization of the Western Mediterranean took place due to the collisions of continental microplates against the passive Iberian and Africa margins. During the Late Miocene a new geodynamic period known as the neotectonic stage (Groupe de Recherches Néotectoniques de l'arc de Gibraltar, 1977) or post-orogenic stage (Viseras *et al.*, 2004) produced the Betic interior basins (*e.g.* Granada, Lorca, and Fortuna) caused by important post-orogenic isostatic readjustments as a consequence of the relative movement between Africa and Europe (plus Iberia). Recent reviews of the chronology of the Betic Cordillera and the Alboran Sea sedimentary basins infill have shown a major time gap in the Early Tortonian (Rodríguez-Fernández *et al.*, 1999; Viseras *et al.*, 2004) registered as an extensive relative sea-level rise (transgressive and highstand phases). The complex network of these basins connected the Atlantic Ocean with the Mediterranean Sea, this being known as the Betic seaway. This seaway was closed during the latest Tortonian (Soria *et al.*, 1999), as has been registered in the Mediterranean affinity Betic basins such as Granada, Lorca, and Fortuna by evaporite precipitation and defined as the Tortonian Salinity Crisis (Krijgsman *et al.*, 2000), prior to the Messinian Salinity Crisis of the deep Mediterranean basin. The Tortonian Salinity Crisis has a clear relation with tectonics as in the Fortuna Basin (Tent-Manclús *et al.*, 2008). In other basins such as Guadix (central Betics), it corresponds to shallow clastic marine units (Soria *et al.*, 2003), or the Bajo Segura Basin by a major lowstand erosional surface (Tent-Manclús *et al.*, 2008).

Due to the relevance of the northern Atlantic-Mediterranean passage closure in the Mediterranean palaeogeographic evolution, the precise dating of the Betic Late Miocene sediments is needed in order to establish a stratigraphic framework for the different basins and thereby provide better knowledge of the progression of the tectonic deformation.

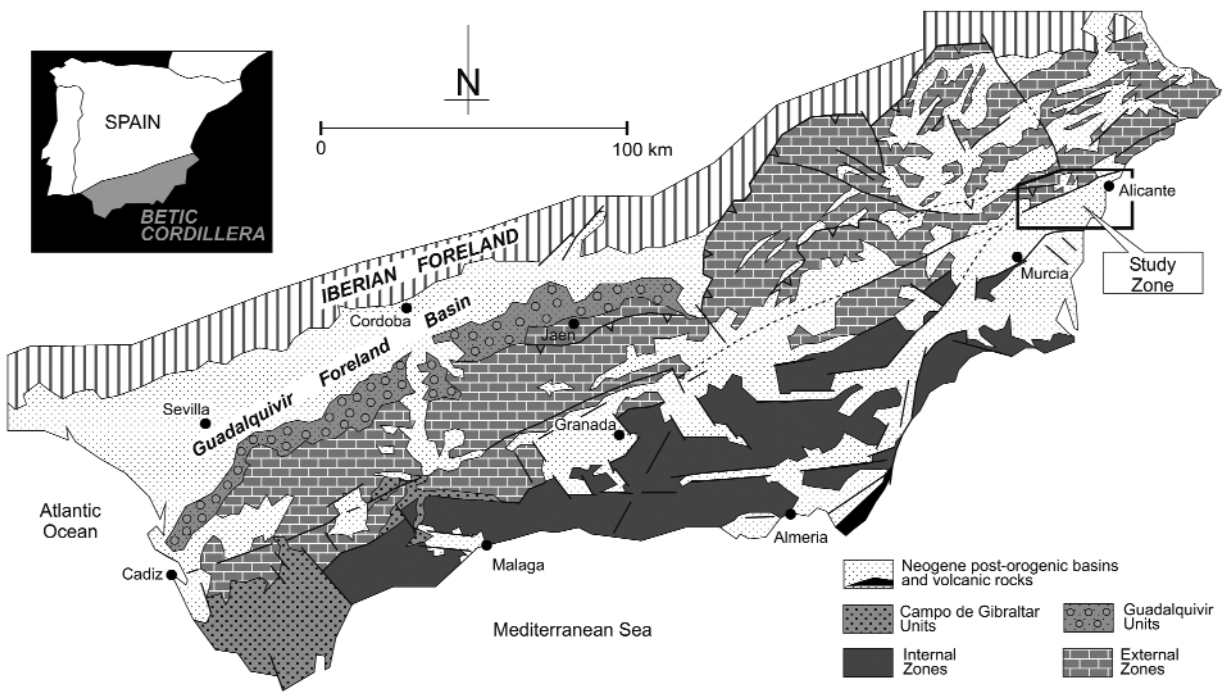

Figure 1. The Betic Cordillera geological sketch.

The aim of this paper is to present a nearly complete marine stratigraphic record of Tortonian age in the Betic Cordillera. This unusual record should allow a better estimate of the timing of the Late Miocene tectonic events. Our technique of smear slides made from centrifugated suspended sediments offers a precise calcareous nannoplankton biostratigraphy of the Tortonian sediments. Also it is completed with the planktonic foraminifera biostratigraphy, providing a more precise biostratigraphic scheme. This study is the first updated chronostratigraphic framework supported by calcareous nannofossils, and planktonic foraminifera bioevents following the tuned scale of Lourens *et al.* (2004), and completed by a magnetostratigraphic study of the Betic Cordillera Tortonian sediments.

2. SAMPLING AND METHODS

The Tortonian sediments are well exposed in two sections distributed along the Crevillente-Abanilla lineation (Fig. 2). The first one, the *Albatera* section is located in the western Alicante province about 8 km north of the Albatera village. It corresponds to a natural section of a creek west of the Albatera-Hondón de los Frailes road (CV-873). The second one, the *Les Moreres* section is located 2 km north of the Crevillente village in the *Les Moreres* valley. In these two sections, the bedding is tilted towards the southeast.

The *Albatera* and *Les Moreres* sections (Fig. 2) have been sampled to study their nannofossil and planktonic foraminifera assemblages. A total of 99 samples were collected, 65 from the *Les Moreres* section (3.5-4 m interval), and 34 from the *Albatera* section (1-1.5 m interval), as shown in Figure 3. Each sample was wet sieved to collect the >63 µm and >125 µm fractions, whereupon the >125 µm fractions were studied. Then, to determine the coiling ratio of *Neogloboquadrina acostaensis*, the samples shown in the Figure 4 were sorted in Chapman slides and more than 200 individual planktonic foraminifera were counted per sample.

For the calcareous nannofossil study, four different smear slides were prepared for each sample, using the following method to increase the nannofossils to silt ratio (Lancis, 1998): For the first smear slide, 0.1 g of sediment was suspended in 10 ml distilled water (pH 7), extending on a 300 mm^2 surface, in one case, the direct suspension (without dilution) and in the other smear slide after a 1/3 dilution of the suspension with distilled water. In order to increase the smear slides quality, a second procedure was performed as follows. A 10-ml suspension of 0.1 g sediment in distilled water (pH 7) was centrifuged at 1800 rpm

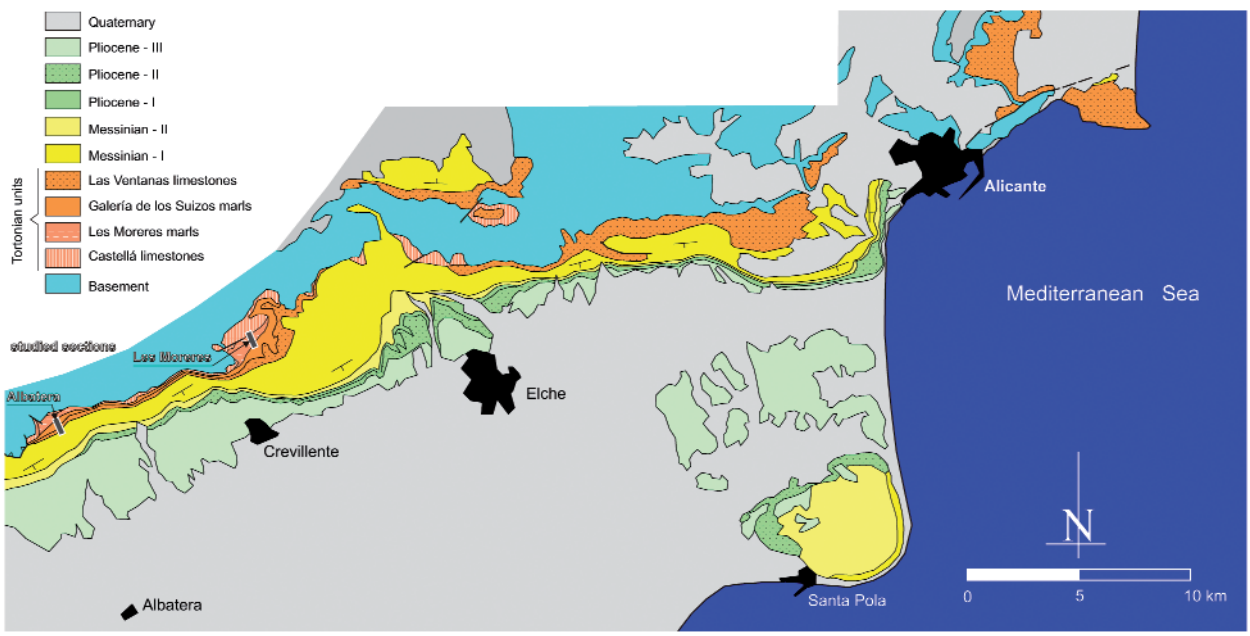

Figure 2. Simplified geological map of the study area with the locations of the *Albatera* and *Les Moreres* sections.

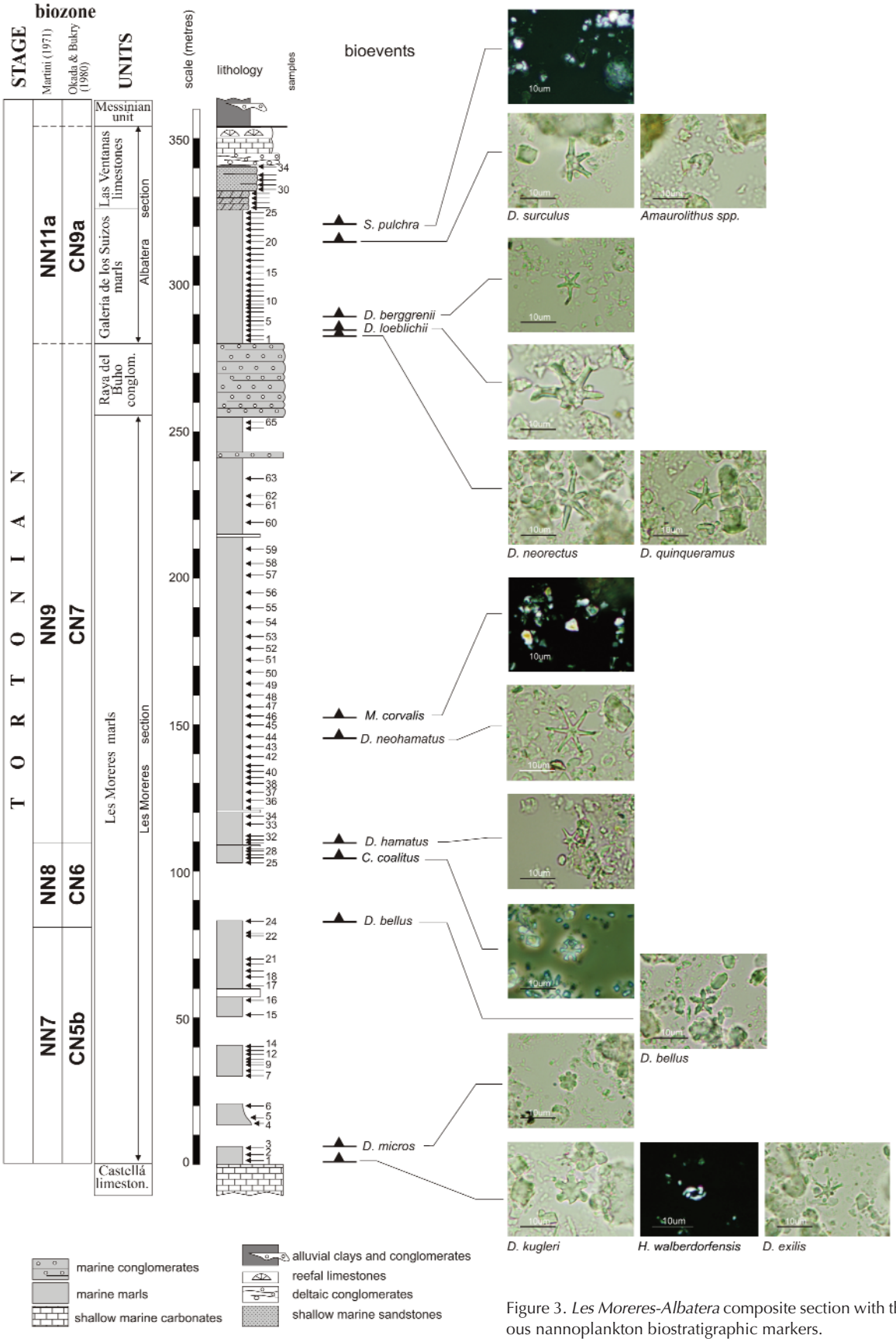

Figure 3. *Les Moreres-Albatera* composite section with the main calcareous nannoplankton biostratigraphic markers.

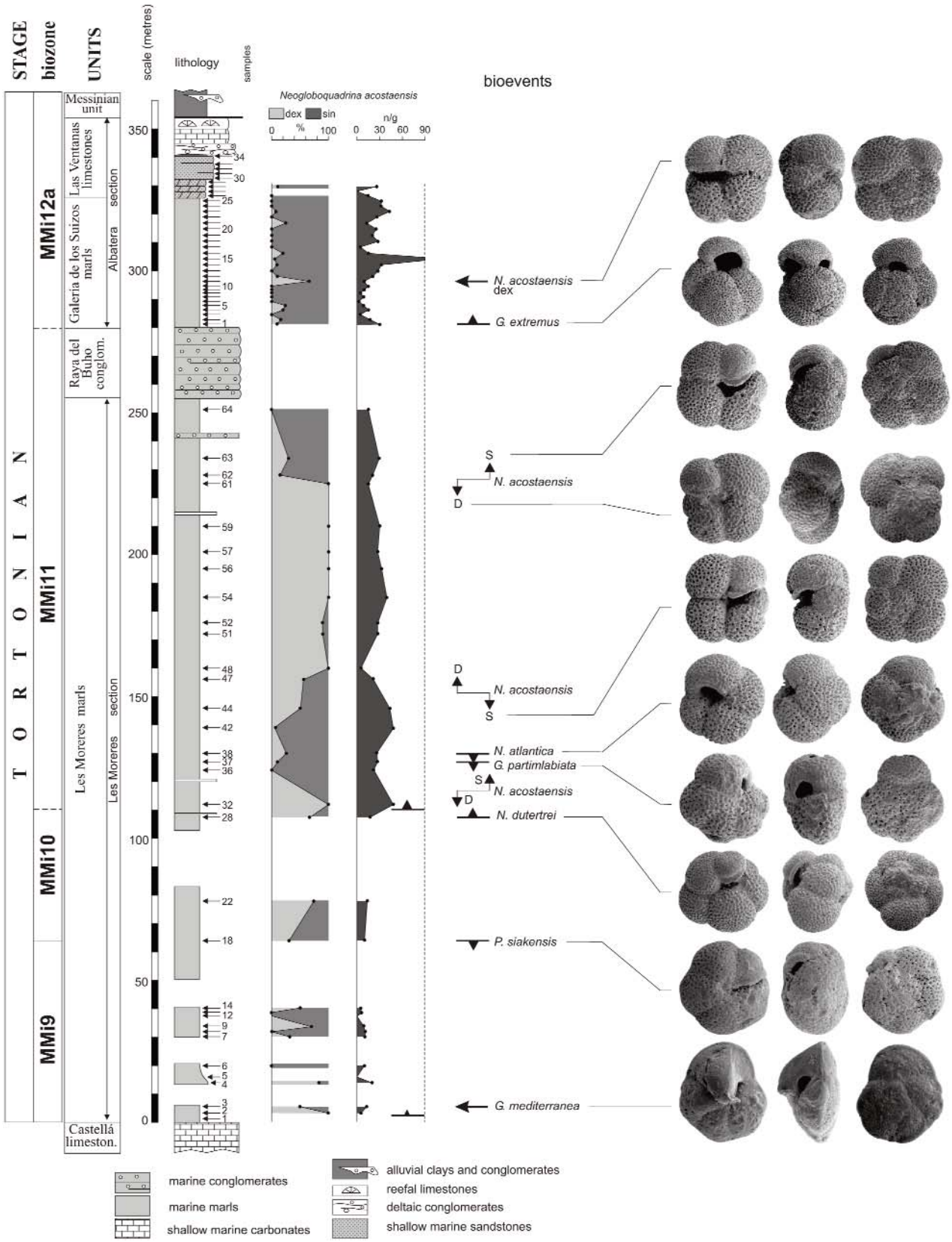

Figure 4. Planktonic foraminifera bioevents in the *Les Moreres-Albatera* composite section. The content of *Neogloboquadrina acostaensis* is expresed as the number of specimens per weight in grams of washed residue (n/g).

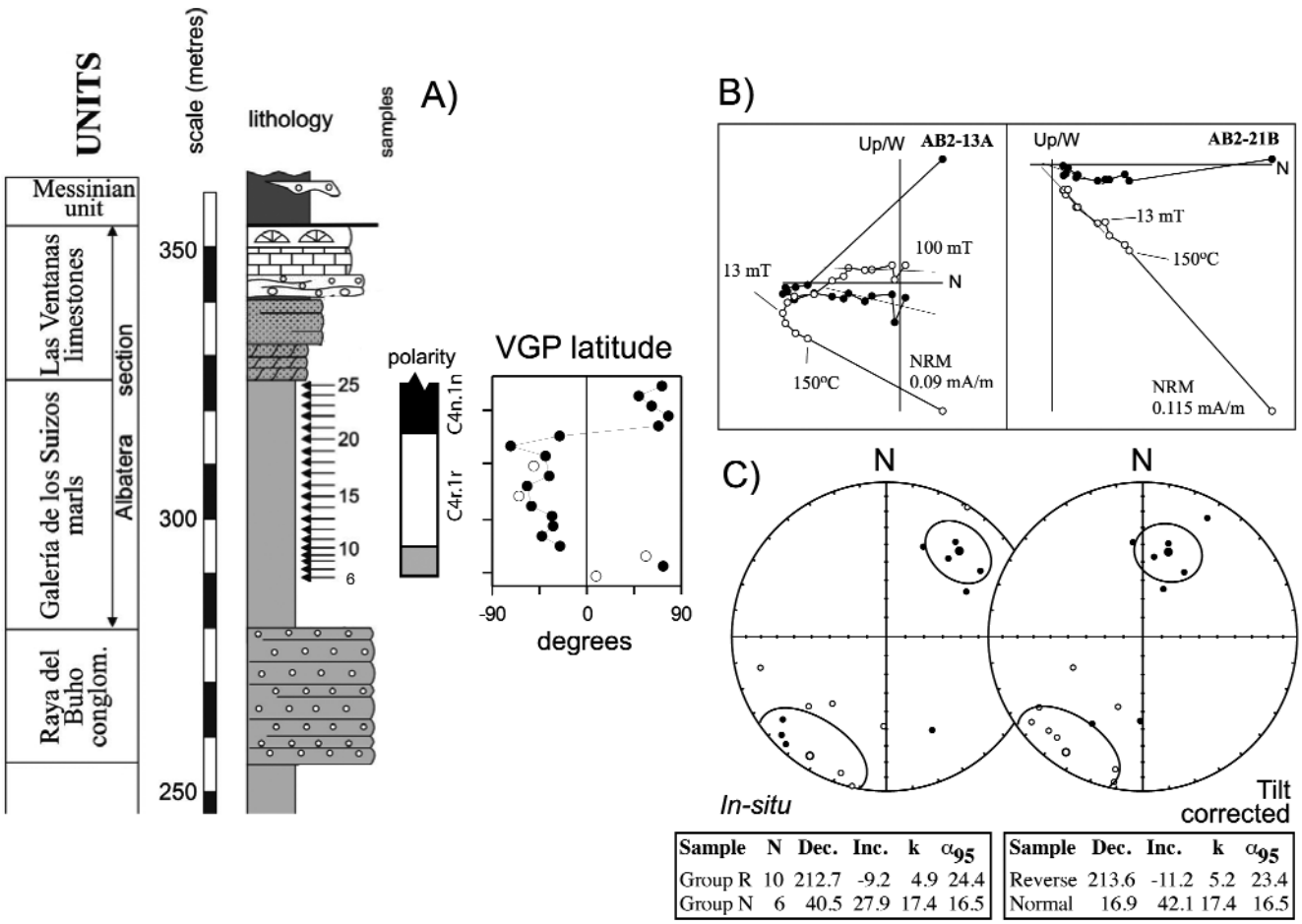

Sample	N	Dec.	Inc.	k	α_{95}
Group R	10	212.7	-9.2	4.9	24.4
Group N	6	40.5	27.9	17.4	16.5

Sample	Dec.	Inc.	k	α_{95}
Reverse	213.6	-11.2	5.2	23.4
Normal	16.9	42.1	17.4	16.5

Figure 5. Paleomagnetic results and magnetostratigraphic interpretation of the *Albatera* section. A) Stratigraphic log and polarity interpretation, VGP (virtual geomagnetic pole) (open circles: class B sites; closed circles: class A sites). B) Examples of orthogonal demagnetization diagrams representative of normal (AB2-21B) and reverse (AB2-13A) samples are given (open and closed symbols denote projections onto the vertical and horizontal planes, respectively). C) Stereographic projections of the ChRM components before (in situ) and after bedding correction (tilt corrected) are shown (open and closed symbols indicate projections onto the upper and lower hemisphere, respectively), together with the mean direction and statistics of normal and reverse polarity directions.

(450 g) for 2 min at room temperature. After discarding the supernatant, distilled water was added to the pellet to achieve 10 ml of suspension, and the new mixture was submitted to sonication for 8 seconds. This centrifugation-sonication procedure was repeated five times. Finally, 0.1 ml of the suspension was directly extended covering a 300 mm^2 surface on the slide, without dilution for the third smear slide and after 1/3 dilution with distilled water (pH 7) for the fourth one.

The four prepared smear slides of each sample were analysed at 100x, scanning the entire slide to find all the rare biostratigraphic markers. The mean values for nannofossil abundance were calculated using the number of coccoliths found in 30 visual fields counting around 500 nannoliths larger than 3 µm (Lancis, 1998). The percentage of *Reticulofenestra pseudoumbilicus* >7 µm was estimated considering only the nannoliths larger than 3 µm. For counting the "small reticulofenestrids" (< 3 µm), mean values were estimated counting around 3000 nannoliths in 30 visual fields and the percentages were calculated considering all the nannoliths. Finally, to determine the abundance of the asteroliths, nannoliths were counted in 600 visual fields. All values were then transformed into the number of nannoliths in 1 mm^2 of slide.

An initial pilot paleomagnetic study along the Les Moreres marls along the *Les Moreres* section indicated that the rocks are very weakly magnetic and unsuitable for magnetostratigraphic purposes. Paleomagnetic sampling was focussed to the more fresh marls after cleaning the outcrop. This study is, therefore, based on a total of 20

unique sampling sites, comprising 1 hand-sample per site from the Galeria de los Suizos Marls along the *Albatera* section (Fig. 5A). Hand-samples were oriented in situ with a compass and subsequently standard cubic specimens were cut in the laboratory for analysis. Natural remanent magnetization (NRM) and remanence through demagnetization were measured on a 2G Enterprises DC SQUID high-resolution pass-through cryogenic magnetometer (manufacturer noise level of 10^{-12} Am^2) operated in a shielded room at the Istituto Nazionale di Geofisica e Vulcanologia in Rome, Italy. A Pyrox oven in the shielded room was used for thermal demagnetizations and alternating field (AF) demagnetization was performed with three orthogonal coils installed inline with the cryogenic magnetometer. Progressive stepwise AF demagnetization was routinely used and applied after a single heating step to 150°C. AF demagnetization included 14 steps (4, 8, 13, 17, 21, 25, 30, 35, 40, 45, 50, 60, 80, 100 mT). Characteristic remanent magnetizations (ChRM) were computed by least-squares fitting (Kirschvink, 1980) on the orthogonal demagnetization plots (Zijderveld, 1967). The ChRM declination and inclination were used to derive the latitude of the virtual geomagnetic pole (VGP) of each sample. This parameter was taken as an indicator of the original magnetic polarity, normal polarity being indicated by positive VGP latitudes and reverse polarity by negative VGP latitudes.

3. STRATIGRAPHY OF THE SOUTHERN ABANILLA-CREVILLENTE LINEATION

The Tortonian sediments studied seal the contact between the two major geological domains of the Betic Cordillera orogen (Fig. 1): the External Zone, the former South Iberian Palaeomargin (to the north), and the Internal Zone or Alborán Block that constitutes an allochthonous lithospheric fragment (Andrieux *et al.*, 1971), dominated by metamorphic rocks (to the south). Rocks from the Internal and External zones can be considered the basement. Over this basement, NW-SE basins formed during the Middle Miocene to the Tortonian (Tent-Manclús, 2003), and then, in the latest Tortonian the onset of the Trans-Alboran Shear Zone changed the palaeogeography developing the SW-NE Bajo Segura Basin (Tent-Manclús *et al.*, 2008). This change is marked by a calcareous sandstone unit including coral-reef patches (Santisteban Bové, 1981), which deepens to the East. This unit was included by Montenat (1977) as the upper part of its Tortonian II unit, and was later named Las Ventanas Limestone by Tent-Manclús (2003).

3.1 Lithostratigraphic units

Montenat (1977) presented the first lithostratigraphic sketch of these basins, establishing over the basement the units: "Tortonian I", to the sediments below the intra-Tortonian discontinuity, the "Tortonian II" to the marine sediments overlying the intra-Tortonian discontinuity, and the "Upper Miocene" to the continental sediments between the marine "Tortonian II" and "Pliocene I" sediments. Subsequently, Montenat *et al.* (1990), Alfaro García (1995), Soria *et al.* (2001), Tent-Manclús (2003), Tent-Manclús *et al.* (2004), and Soria *et al.* (2005) used many alternative lithological units, the relations of which are shown in Figure 6. For Montenat (1977) the older sediments over the basement in the southern flank of the Crevillente-Abanilla lineation were assigned to the Tortonian II unit. A brief description of the lithological units used in this study is provided below.

a) El Castellà Limestone: dark grey to reddish bioclastic limestones.
b) Les Moreres Marls: 300-m-thick white marls with some detrital intercalations near its bottom.
c) Raya del Búho Conglomerate: a marine unit formed by balanid-encrusted metamorphic clasts of Internal Zone provenance, which in some outcrops erode the Moreres Marls.
d) Galería de los Suizos Marls: a marly marine unit containing planktonic microfossils upwardly increasing in carbonate content.
e) Las Ventanas Limestone: coral-reef limestone and yellowish calcareous sandstone, containing abundant fossils of corals (*Porites* and *Tarbellastrea*), bivalves, red algae, equinoderms, and *Dentalium*; laterally, this unit thins and disappears to the western Fortuna Basin (Azema and Montenat, 1975).
f) Unconformably overlying the Las Ventanas limestone unit appears patches of marine conglomerates with clasts of the Crevillente Sierra sequences (External

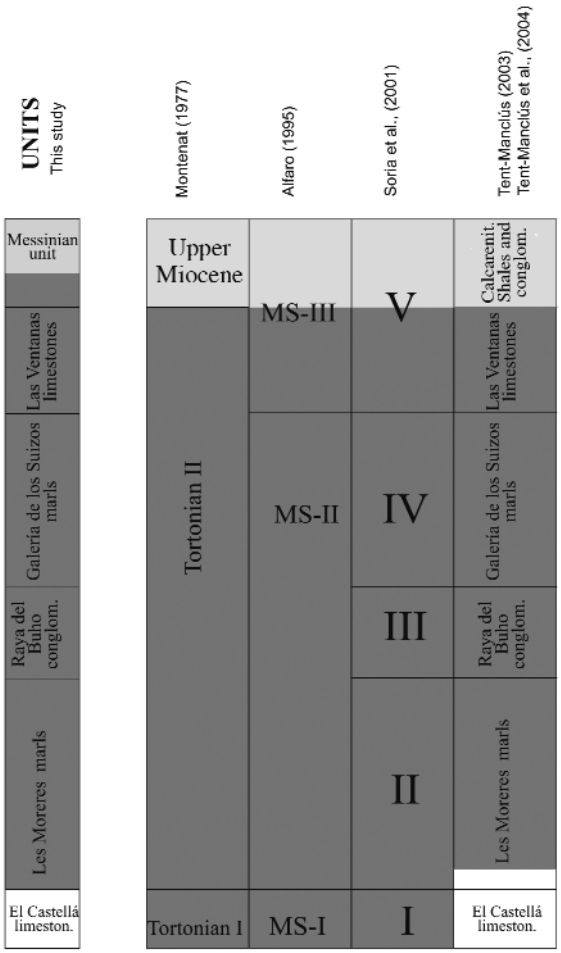

Figure 6. The rock units names used by earlier works and the equivalences with the ones used in this study. The darker and light gray and white backgrounds are relative to the age assignment in the different works. The Tortonian deposits are in darker gray than the Messinian and the white background is the Serravallian assigned ages.

Zone and underlying tertiary) and some coral-reef which indicate the erosion of the Las Ventanas reef. Finally, at the top of the section is covered by a Messinian unit made by continental red beds.

4. BIOSTRATIGRAPHY OF CALCAREOUS NANNOFOSSILS

The nannofossil assemblages came from the two marly lithostratigraphic units, Les Moreres and Galería de los Suizos Marls. Figure 3 shows the main biostratigraphic events in the Tortonian age sediments studied. The preservation is fairly good and reworked nannoliths from the Early Miocene, Paleocene, and Late Cretaceous are frequent.

4.1 Les Moreres Marls

The lowest levels of the Les Moreres Marls contain the following main calcareous nannoplankton assemblages: *Discoaster kugleri* (Fig. 7-1; 7-2; 7-3), *D. exilis* (Fig. 7-5; 7-6), *D. aulakos, D. micros* (Fig. 7-7), *D. prepentaradiatus, Coccolithus miopelagicus, C. pelagicus, Calcidiscus* spp., *Sphenolithus abies, Helicosphaera carteri, H. walberdorfensis* (Fig. 7-4) *Umbilicosphaera rotula, Dictyococcites antarcticus, Reticulofenestra pseudoumbilicus* (Fig. 7-9), *R. haqii, R. minutula,* and abundant "small reticulofenestrids" (*Reticulofenestra minuta* and *Dictyococcites productus*).

In the middle part of the *Les Moreres* section, sample 26, appear the first specimens of *Catinaster coalitus* (Fig. 7-8) and *Discoaster bellus* (Fig. 7-10, 7-11). In sample 31 the first *D. hamatus* (Fig. 7-12) was found, while *D. kugleri* and *H. walberdorfensis* had dissapeared. Scarce specimens of *Discoaster calcaris, D. neohamatus*, and *D. pseudovariabilis* were also present and became more abundant in the upper part of the *Les Moreres* section. The first *Minilitha convalis* (Fig. 7-13, 7-14) were detected in the sample 46. The broken and overgrowth of nannofossils indicate some reworking in the samples.

4.2 Galería de los Suizos Marls

The lowest levels of the Galería de los Suizos Marls contain the following nannofossil assemblage: *Coccolithus pelagicus, Umbilicosphaera rotula, Calcidiscus macintyrei, C. leptoporus, Discoaster quinqueramus* (Fig. 8-4), *D. brouweri* (Fig. 8-1), *D. neorectus* (Fig. 8-3), *D. variabilis* (Fig. 8-8), *D. calcaris, D. pentaradiatus, D. pseudovari-*

Figure 7. **1-3-** *Discoaster kugleri* Martini & Bramlette, parallel light (PL): **1** sample 12 of *Les Moreres* section (Mor); **2** sample 19 Mor; **3** sample 22 Mor. **4**- *Helicosphaera walbersdorfensis* Müller, crossed nicols (XN), sample 1 Mor. **5-6**- *Discoaster exilis* Martini & Bramlette, PL: **5** sample 22 Mor; **6** sample 1 Mor. **7**- *Discoaster micros* Theodoridis, PL, sample 20 Mor. **8**- *Catinaster coalitus* Martini & Bramlette, PL, sample 27 Mor. **9**- *Reticulofenestra pseudoumbilicus* Gartner, XN, sample 52 Mor. **10-11**- *Discoaster bellus* Bukry & Percival, PL: **10** sample 25 Mor; **11** sample 43 Mor. **12**- *Discoaster hamatus* Martini & Bramlette, PL, sample 60 Mor. **13-14.**- *Minylitha convallis* Bukry, sample 2 *Albatera* section (AB); **13** PL; **14** XN. **15-** *Discoaster neohamatus* Bukry & Bramlette, PL, sample 2 AB.

Figure 7

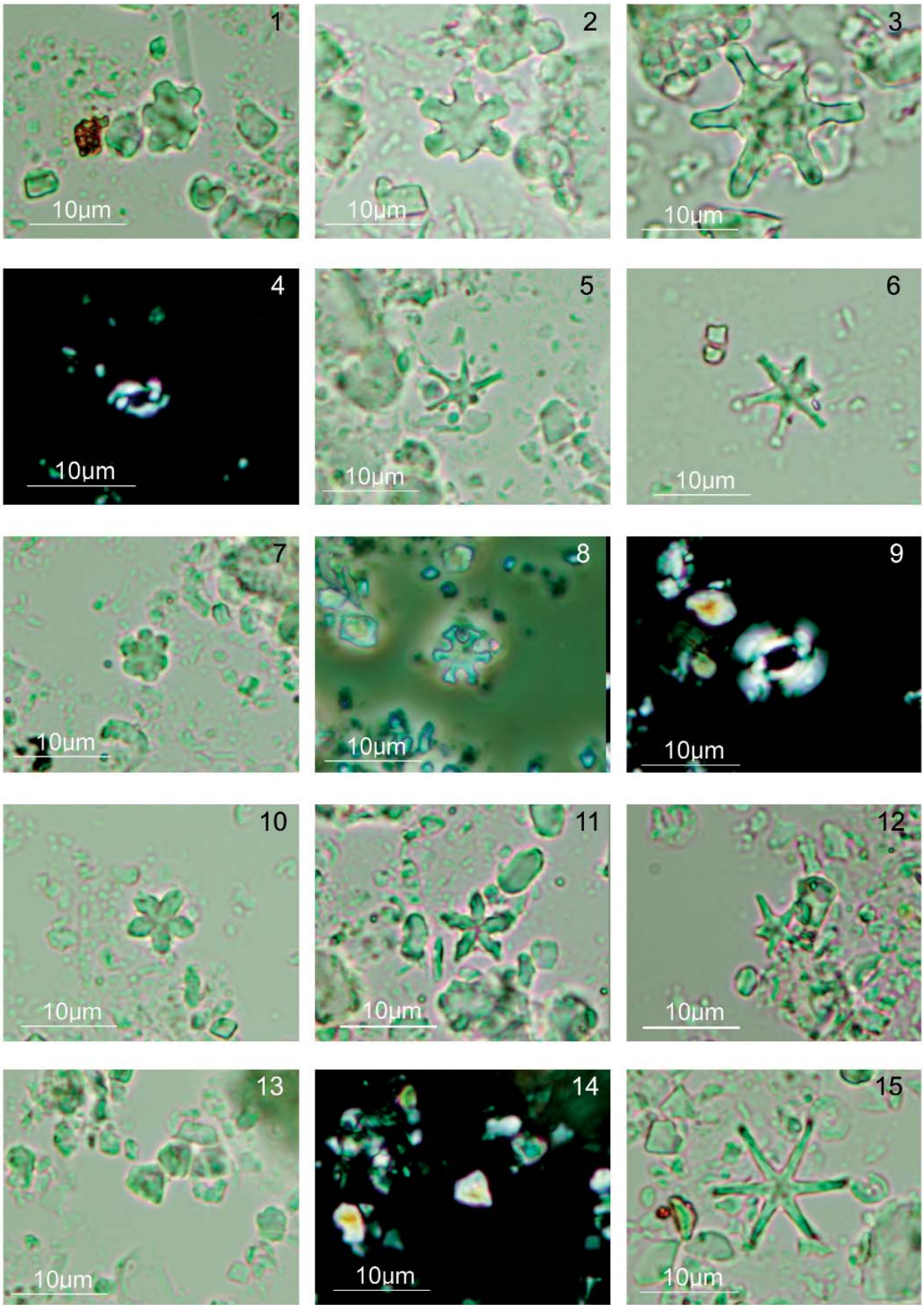
1
10µm
2
10µm
3
10µm
4
10µm
5
10µm
6
10µm
7
10µm
8
10µm
9
10µm
10
10µm
11
10µm
12
10µm
13
10µm
14
10µm
15
10µm

abilis, D. loeblichii, D. intercalaris (Fig. 8-11), *D. berggrenii* (Fig. 8-6), *Minilitha convalis* (Fig. 8-13; 8-14) *Sphenolithus abies*, *Sph. neoabies,* and *Scyphosphaera apsteinii* (Fig. 8-5). *Reticulofenestra pseudoumbilicus* > 7 µm, though present in almost all the samples of the *Albatera* section, represents less than 5% of the assemblage. *R. pseudoumbilicus* 5-7 µm, *R. haqii*, and *R. minutula* are also abundant and the "small reticulofenestrids" (*Reticulofenestra minuta* and *Dictyococcites productus*) show high percentages that in some cases approach 70%. In the highest part of the *Albatera* section, we found *Scyphospahaera intermedia* (Fig. 8-9), *Scy. conica* (Fig. 8-7), *Scy. amphora* (Fig. 8-10) and abundant *Pontosphaera multipora*. The first appearance of *Discoaster surculus* is in sample 15 but its First Common Occurrence (FCO) is from the sample 22 upwards. Some initial forms of *Amaurolithus* cf. *primus* were found in samples 20 and 23 (Fig. 8-13; 8-14) together with *Syracosphaera pulchra* (Fig. 8-15).

5. BIOSTRATIGRAPHY OF PLANKTONIC FORAMINIFERA

The Late Miocene planktonic foraminiferal microfossils in *Les Moreres* and the *Albatera* sections are mixed with a variable number of reworked Paleogene and Lower-Middle Miocene planktonic foraminifera. Preservation is fairly good both for the Late Miocene and reworked specimens. Washed residues in the 125-µm fraction were used to portray presence of Late Miocene marker species, in addition to the coiling patterns of *Neogloboquadrina acostaensis* (Fig. 4). In this study, we have considered the most typical species included in recent astronomically-calibrated biozonation charts, as that proposed by Lourens *et al*. (2004). Below, we follow the biozones established by these authors in order to describe the biostratigraphy of the studied section.

5.1 Les Moreres section

The first significant biostratigraphic horizon in the Les Moreres Marls is the LCO (Last Common Occurrence) of *Paragloborotalia siakensis* in sample 18, marking the upper boundary of the MMi9 biozone. *Neogloboquadrina acostaensis* is present from the extreme base to the top of the section; its content increases and is regularly recorded upward in sample 32, where the FCO of this species is located, marking the boundary between MMi10 and MMi11 biozones. From sample 32 to the top, the section can be assigned to the MMi11 biozone. Several noticeable intra-zonal bioevents are unambiguously correlated with other classical Mediterranean sections (*e.g.* the *Gibliscemi* composite section in Sicily; Hilgen *et al*., 2000). These events, from the bottom to the top of the biozone, are: 1) the dextral to sinistral coiling change of Neogloboquadrinids between samples 32 and 36; 2) the LCO of *Globorotalia partimlabiata* in sample 37; 3) the LCO of *Neogloboquadrina atlantica* (large- and small-sized forms) in sample 38; 4) the sinistral to dextral coiling change of *Neogloboquadrina acostaensis* between samples 44 and 47; and 5) the dextral to sinistral coiling change of *Neogloquadrina acostaensis* between samples 59 and 61. This last event is located below and very close of the stratigraphic boundary between the Les Moreres Marls and the Raya del Búho Conglomerate. Also, it bears noting a brief influx of *Globorotalia mediterranea* at the base of the Les Moreres Marls, inside the MMi9 biozone. This constitutes the first report of this species in any Mediterranean section during the earliest Tortonian (Fig. 4).

5.2 Albatera section

From the bottom to the top of the Galería de los Suizos Marls, *Globigerinoides extremus* appears regularly; in addition, the joint presence of this species with dominant sinistral forms of *Neogloboquadrina acostaensis*, indicate the MMi12a biozone. In the lower half of this biozone (sample 11) an influx (ca. 70%) of dextral *Neogloboquad-*

Figure 8. **1**- *Discoaster brouweri* (Tan) Bramlette & Riedel, PL, sample 7 *Albatera* section (AB). **2-***Discoaster loeblichii* Bukry, PL, sample 22 AB. **3-** *Discoaster neorectus* Bukry, PL, sample 15 AB. **4**- *Discoaster quinqueramus* Gartner, PL, sample 15 AB. **5**- *Scyphosphaera apsteinii* Lohmann, PL, sample 7 AB. **6-** *Discoaster berggrenii* Bukry, PL, sample 23 AB. **7**- *Scyphosphaera conica* Kamptner, PL, sample 22 AB. **8**- *Discoaster variabilis* Martini & Bramlette, PL, sample 15 AB. **9**- *Scyphosphaera intermedia* Deflandre, PL, sample 17 AB. **10-** *Scyphosphaera amphora* Deflandre, PL, sample 22 AB. **11-** *Discoaster intercalaris* Bukry, PL, sample 12 AB. **12**- *Discoaster surculus* Martini & Bramlette, PL, sample 22 AB. **13-14**- *Amaurolithus* spp. (*A.* cf. *primus*) (Bukry & Percival) Gartner & Bukry; **13** PL, sample 20 AB; **14** PL, sample 23 23. **15-** *Syracosphaera pulchra* Lohmann, XN, sample 23 AB.

Figure 8

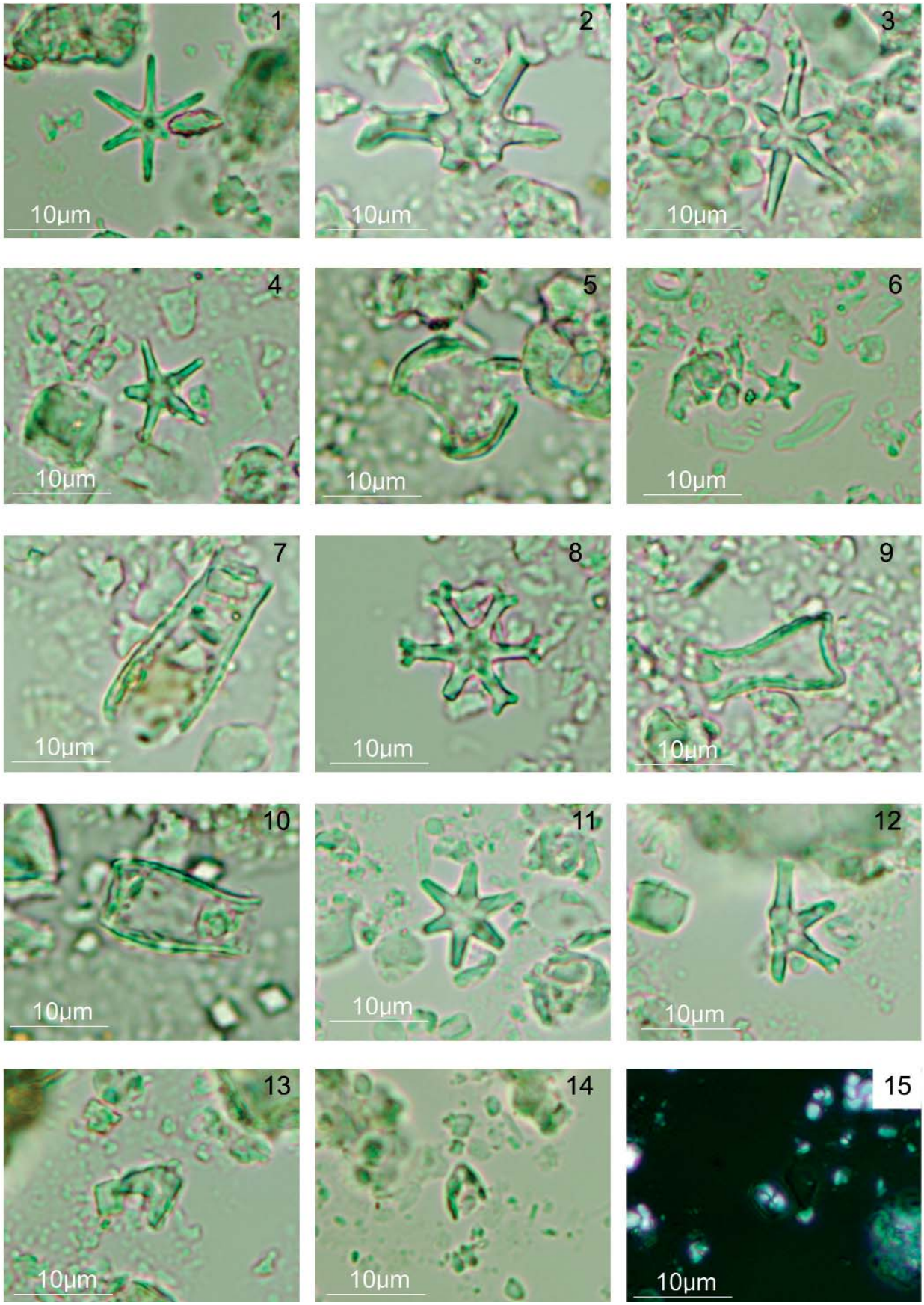
1
10µm
2
10µm
3
10µm
4
10µm
5
10µm
6
10µm
7
10µm
8
10µm
9
10µm
10
10µm
11
10µm
12
10µm
13
10µm
14
10µm
15
10µm

rina acostaensis occurs. This is a new and unreported event, until the present, in the Mediterranean Tortonian sections. The Las Ventanas Limestone, overlying the Galería de los Suizos Marls, contains no significant biostratigraphic planktonic foraminifera.

6. CALCAREOUS NANNOFOSSILS EVENTS

The distribution patterns of the selected calcareous nannofossil species are shown in the Figures 9, 10, 11, and 12. Most of them are index species for the Middle and Late Miocene in the Mediterranean and in the low-latitude oceans. The asteroliths are scarce and its preservation is poor in the *Les Moreres* section and best preserved in the *Albatera* section, Galeria de los Suizos Marls. The occurrences and distribution patterns of the most important species are discussed bellow.

6.1 Presence of *Discoaster kugleri*

Bukry (1973) suggested as the secondary criterion of definition of the boundary CN5b/CN6 the LO (Last Occurrence) of *D. kugleri* join with the FO (First Occurrence) of *C. coalitus*. In addition, Zone CN5 is divided into two subzones (CN5b and CN5a) by the FO de *D. kugleri* (Bukry, 1973), which also defines the NN7/NN6 (Martini, 1971) zonal boundary. The recognition of this boundary has been debated, as *D. kugleri* is considered by many authors to be a weak marker (Gartner, 1992; Fornaciari *et al*., 1990; Raffi & Flores, 1995; Fornaciari *et al*., 1996). Although its interval of abundance has a wide geographic distribution (Raffi *et al*., 1995; Backman & Raffi, 1997), *D. kugleri* is generally rare in the Mediterranean (Müller, 1978), and therefore it is not included as a (sub)zonal marker in the Middle Miocene Mediterranean zonation by Fornaciari *et al*. (1996).

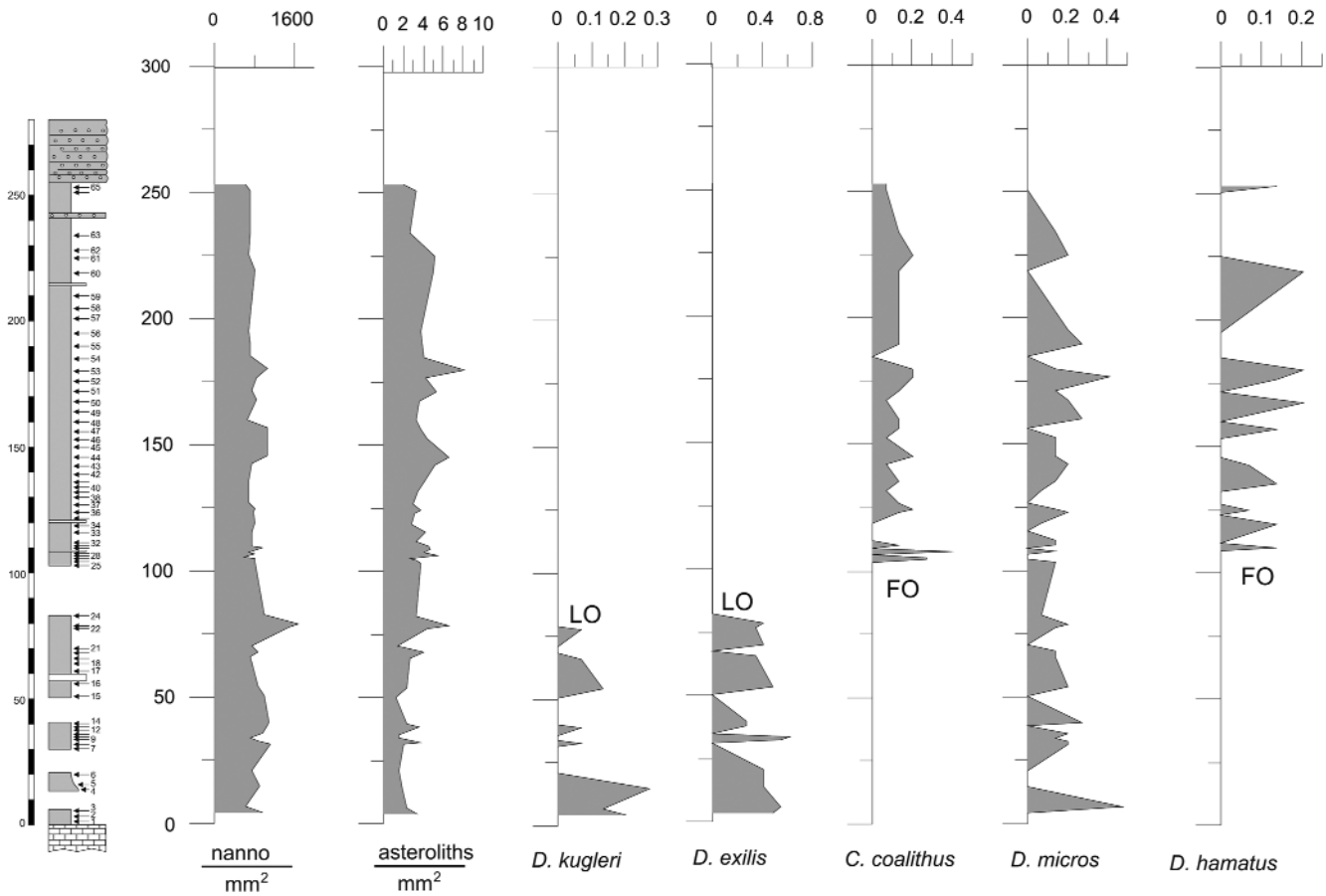

Figure 9. Quantitative distribution pattern of selected nannofossils in the *Les Moreres* section (as number of specimens per mm^2). The following acronums indicate bioevents: FO (First Occurrence); LO (Last Occurrence); FCO (First Common Occurrence); LCO (Last Common Occurrence). Please note differences in scaling.

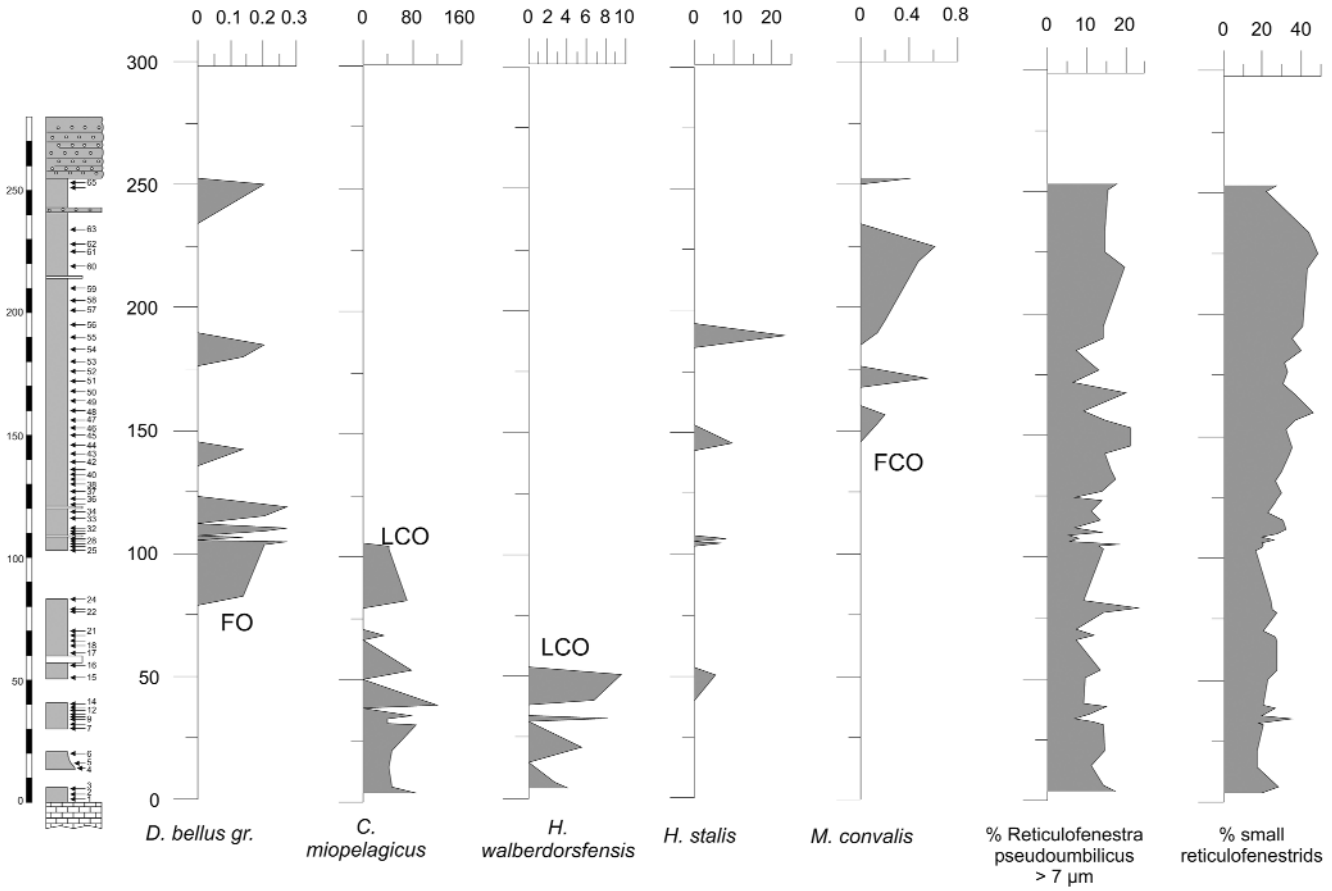

Figure 10. Quantitative distribution pattern of selected nannofossils in the *Les Moreres* section (as number of specimens per mm^2). The following acronums indicate bioevents: FO (First Occurrence); LO (Last Occurrence); FCO (First Common Occurrence); LCO (Last Common Occurrence). Please note differences in scaling.

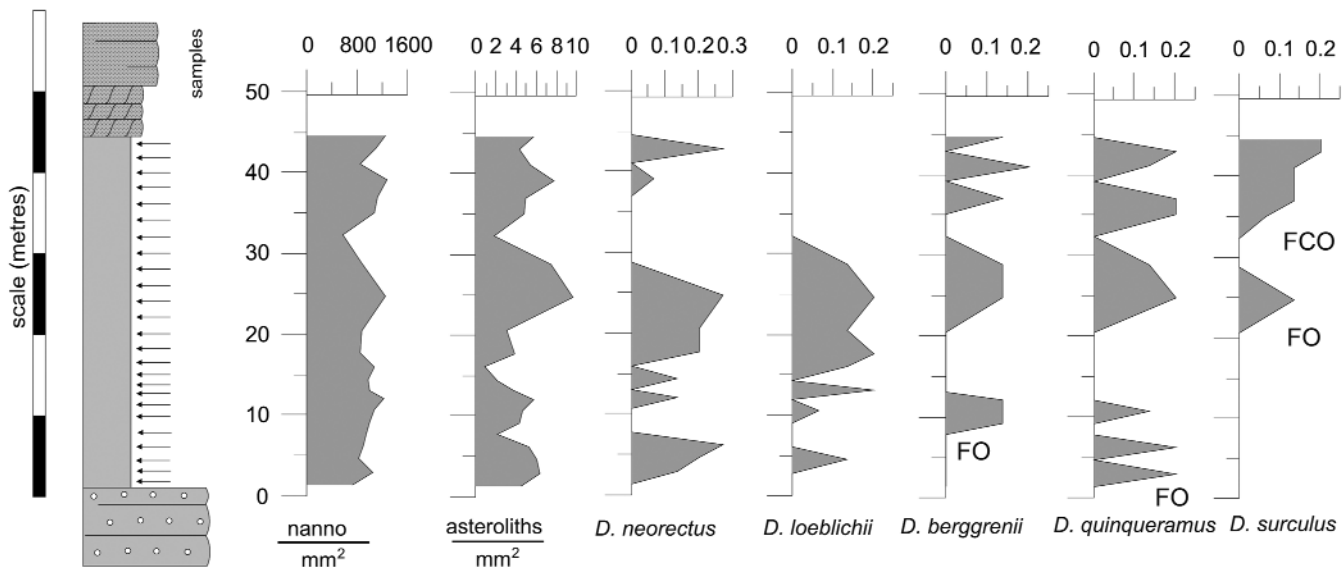

Figure 11. Quantitative distribution pattern of selected nannofossils in the *Albatera* section (as number of specimens per mm^2). The following acronums indicate bioevents: FO (First Occurrence); LO (Last Occurrence); FCO (First Common Occurrence); LCO (Last Common Occurrence). Please note differences in scaling.

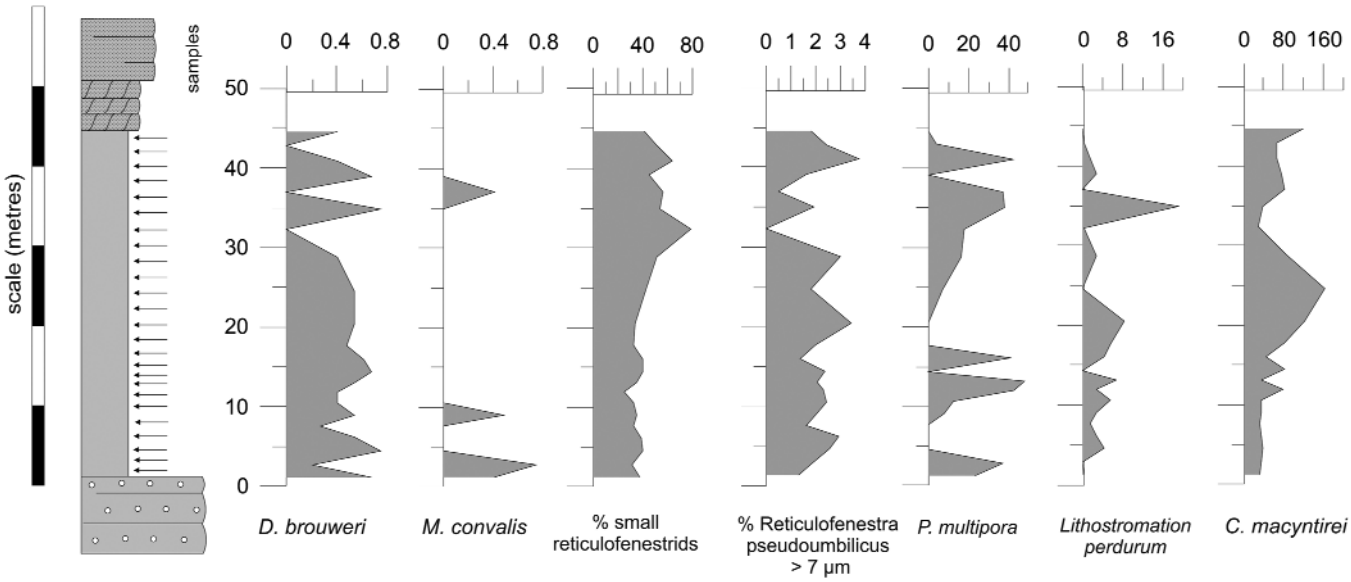

Figure 12. Quantitative distribution pattern of selected nannofossils in the *Albatera* section (as number of specimens per mm^2). The following acronums indicate bioevents: FO (First Occurrence); LO (Last Occurrence); FCO (First Common Occurrence); LCO (Last Common Occurrence). Please note differences in scaling.

However, Hilgen *et al*. (2000), Hilgen *et al*. (2003), Foresi *et al*. (2002), Caruso *et al*. (2002) in the results of the analyses on the high-resolution samples of the Mediterranean basin show that the biostratigraphic signal provided by *D. kugleri* is clear and both the FCO and LCO are easily identified with astronomical ages also coincident with the same events in the low-latitude open oceans. In the western equatorial Atlantic, ODP sites 925 and 926 the FCO and LCO of *D. kugleri* were astronomically calibrated and dated at 11.863 and 11.578 Ma, respectively (Backman & Raffi, 1997; Shackleton & Crowhurst, 1997; Lourens *et al*., 2004).

In the *Les Moreres* section, *D. kugleri* is scarce in the lowest samples, appears sporadically and then disappears before the FO of *Catinaster coalithus*. We cannot determine whether we are in the interval of continuous presence below the LCO or just above this level, which marks the Serravallian-Tortonian boundary.

6.2 LO of *Discoaster exilis*

Raffi *et al*. (1995) showed that the *D. exilis* LO occurs in an interval encompassing the appearance level of *D. hamatus* (between the top of biozone CN6 and the lowermost part of Zone CN7) being an event controlled by environmental conditions and biogeography. Hilgen *et al*. (2000) in the Mediterranean found a distribution of *D. exilis* coincident with the data of the western equatorial Atlantic of Raffi *et al*. (1995). The distribution of *D. exilis* in *Les Moreres* section show a parallel distribution with *D. kugleri*, although the former is more abundant but seems to disappear just below the FO of *C. coalithus.*

6.3 LCO of *Helicosphaera walbersdorfensis* and FCO of *H. stalis*

In the *Les Moreres* section, *Helicosphaera walberdorfensis* is present from the bottom of the section to sample 22. Although it is scarce, it coincides in distribution with *D. kugleri* and *D. exilis*. Hilgen *et al*. (2000) in the Mediterranean section of *Gibliscemi* found the LCO of *H. walberdorfensis* coinciding with the FCO of *H. stalis*, having an astronomically tuned age of between 10.743 and 10.717 Ma in agreement with the distributions reported by Fornaciari *et al*. (1996). In our samples, *H. stalis* is even scarcer than *H. walberdorfensis*, so that we could not specify the precise coincidence of the two events. *H. stalis* appears sporadically until the sample 55 of the *Les Moreres* section.

6.4 Presence of *Discoaster micros* and *Catinaster coalitus*

The bottom of the CN6 biozone (Okada & Bukry, 1980) and NN8 biozone (Martini, 1971) is defined by the FO of *C. coalitus* plus the LO of *D. kugleri*. *Catinaster coalitus* is consistently present in the low-latitude assemblages, whereas for Theodoridis (1984) and Fornaciari *et al*. (1996), it is scattered to absent at mid-latitudes and in the Mediterranean. However, Hilgen *et al*. (2000) observed in the Mediterranean *Gibliscemi* section *C. coalitus* in two short intervals join with *D. micros*. Their astronomically tuned FO at 10.738 Ma is consistent with the data from the western equatorial Atlantic at 10.886 Ma (Backman & Raffi, 1997; Raffi *et al*., 2006). In the investigated material, representatives of *Catinaster coalitus* (Fig. 7-8) are scarce but with a quite regular distribution between the samples 26 and 65 of the *Les Moreres* section. *Discoaster micros* (Fig. 7-7), a discoasterid from which the genus *Catinaster* is considered to have evolved (Raffi *et al*., 1998), is also scarce and has a similar distribution. Integrated forms have also been found.

6.5 LCO of *Coccolithus miopelagicus*

The LCO of *C. miopelagicus* has been documented in the Mediterranean where the species is well represented. Fornaciari *et al*. (1996) found this event just below the disappearance level of *H. walberdorfensis*. Hilgen *et al*. (2000) consider LCO of *C. miopelagicus* coincident with the *D. hammatus* first occurrence. In the *Les Moreres* section we have found the LCO of *C. miopelagicus* just above the disappearance of *H. walberdorfensis* and the appearance of the first forms of *D. bellus* and slightly below the appearance of the first *D. hamatus.*

6.6 Presences of *Discoaster bellus, Discoaster hamatus, Discoaster calcaris* and *Discoaster neohamatus*

The appearances of the distinctive Neogene discoasterids *D. bellus* and *D. hamatus* (Fig. 7-10; 7-11; 7-12) constitute an important event that has been used in the open-ocean and Mediterranean biozones. *D. hamatus* is a marker of both standard as well as Mediterranean zonation and its first and last occurrence define the bottom and top of the standard biozones NN9/CN7.

In the Indian Ocean, the two events (FO *D. bellus* gr. and FO *D. hamatus*) mainly coincide (Rio *et al*., 1990). However, in the equatorial Pacific and western equatorial Atlantic, *D. bellus* gr. FO slightly precedes *D. hamatus* (Raffi *et al*., 1995; Backman & Raffi, 1997; Raffi *et al*., 2006). In the western equatorial Atlantic, *D. hamatus* FO was astronomically calibrated at 10.476 by Backman & Raffi, (1997) and afterwards re-tuned by Lourens *et al*. (2004) at 10.549. Hilgen *et al*. (2000) found *D. hamatus* sporadically in the Mediterranean *Gibliscemi* section, assigning a 10.150 Ma age for the FO then recalibrated by Lourens *et al*. (2004) at 10.184 Ma. *Discoaster hamatus* is a scarce and discontinuous form in the *Les Moreres* section between samples 31 to 65, and also *D. bellus* between samples 24 to 64.

Discoaster neohamatus is also very scarce in both sections. Its FO is in the sample 44 of *Les Moreres* section, and its LO in the *Albatera* section is in sample 15. *Discoaster calcaris* also shows a similar distribution. *D. neohamatus* FO is a distinct event in some oceanic areas where the species is well represented and has been established in the western equatorial Atlantic at 10.521 Ma (Backman & Raffi, 1997; Lourens *et al*., 2004; Raffi *et al*., 2006). Hilgen *et al*. (2000) found rare sporadic specimens in the upper part of the Mediterranean *Glibiscemi* section with an astronomically tuned age of 9.867 (Lourens *et al*., 2004; Raffi *et al*., 2006).

6.7 *Minylitha convallis* distribution range

The biostratigraphic significance of *M. convallis* has been documented in different deep-sea successions (Rio *et al*., 1990; Gartner, 1992; Raffi *et al*., 1995; Backman & Raffi, 1997) including the Mediterranean (Theodoridis, 1984; Fornaciari *et al*., 1996; Hilgen *et al*., 2000; Raffi *et al*., 2003). The FO is slightly diachronic with an astronomically tuned age in the Mediterranean, of 10.733 Ma in *Gibliscemi* section (Hilgen *et al*., 2000) and 9.379 Ma in *Metochia* section, (Raffi *et al*., 2003) and with a distribution range until the 8.685 Ma (Hilgen *et al*., 1995; Raffi *et*

al., 2003; Lourens *et al.*, 2004; Raffi *et al.*, 2006). This range is shorter in the Mediterranean than in the tropical Indian Ocean, eastern equatorial Pacific and North Atlantic (Raffi *et al.*, 2003; Lourens *et al.*, 2004; Raffi *et al.*, 2006).

The species characterizes the assemblages of Zones NN9 upper part/CN7b and NN10/CN8. *Minylitha convallis* appears in the sample 46 of the *Les Moreres* section and is found continuously until the sample 2 of the *Albatera* section, after which it appears sporadically until the sample 21 of the *Albatera* section.

6.8 *Discoaster loeblichii* and D. *neorectus* distribution ranges

The FO of *D. loeblichii* and the FO of *D. neorectus* were two events used by Bukry (1973) to divide biozone CN8 into two subzones (CN8a and CN8b). *Discoaster loeblichii* is consistently present in sediments of Late Miocene age at low-latitude sites in the Pacific and in the mid-latitude Atlantic (from chron C4r to C4n/C3Bn reversal) (Bukry, 1971; Bukry, 1973; Gartner, 1992; Raffi *et al.*, 1995; Raffi & Flores, 1995). In the Mediterranean these are rare but have been registered in different sections (Theodoridis, 1984; Martín-Pérez, 1997; Lancis *et al.*, 2010) within the biozones CN8b and CN9a for *D. loeblichii* (Lancis *et al.*, 2010) and lasting to the biozone CN9b for *D. neorectus* (Martin-Perez, 1997; Lancis, 1998; Lancis *et al.*, 2010).

6.9 Paracme interval of *Reticulofenestra pseudoumbilicus*

The quantitative evaluation of the *R. pseudoumbilicus* abundance in the composite section *Les Moreres-Albatera* enabled us to recognize the "Paracme interval", from the bottom of the *Albatera* section, with percentages lower than the 5% in almost all the samples (Raffi *et al.*, 2003). This event, an interval of almost total absence of large specimens (>7µm) of *R. pseudoumbilicus,* was found for the first time by Rio *et al.* (1990) in the Late Miocene sediments from the tropical Indian Ocean. It was soon observed in other oceanic basins (Gartner, 1992, Raffi & Flores, 1995; Backman & Raffi, 1997) and in the Mediterranean, though not as clearly defined as in oceanic areas due to the abundance of reworked forms (Lancis, 1998; Raffi *et al.*, 2003; Lancis *et al.*, 2010). The PB (Paracme Begin) has been astronomically calibrated in the western equatorial Atlantic at 8.785 Ma (Backman & Raffi, 1997; Lourens *et al.*, 2004; Raffi *et al.*, 2006) and in the Mediterranean *Metochia* section at 8.761 Ma (Raffi *et al.* 2003).

6.10 FO of the *Discoaster quinqueramus-Discoaster berggrenii*

The appearance of the species *D. berggrenii* and *D. quinqueramus* corresponds to the biostratigraphic boundary CN8/CN9 (Okada & Bukry, 1980) NN10/NN11 (Martini, 1971). These pentaradiated discoasterids are abundant in the open oceans. In the Mediterranean, they are absent in the sediments of the eastern area (Theodoridis, 1984; Raffi *et al.*, 2003) but can be recognized in the western (Rio *et al.*, 1976; Müller, 1978; Mazzei, 1985; Müller, 1990; Flores *et al.*, 1992; Martín Pérez, 1997; Lancis, 1998; Lancis *et al.*, 2010). The astronomically tuned age for the FO of *D. berggrenii* at the western equatorial Atlantic is 8.29 Ma (Backman & Raffi, 1997; Lourens *et al.*, 2004). *Discoaster berggrenii* and *D. quinqueramus* are scarce but continuous in our samples the FO of *D. quinqueramus* is in the sample 2 of the *Albatera* section and the FO of *D. berggrenii* is in the sample 3 but due to its scarcity both FO could be considered synchronous.

6.11 Bottom of the acme of "small reticulofenestrids"

This event is determined by an increase in the assemblage of small reticulofenestrids (having the long axis smaller than 3 m) including *Reticulofenestra minuta* and *Dictyococcites productus* specimens. This assemblage has been observed by many authors (Backman, 1978; Flores, 1985; Flores & Sierro, 1987; 1989; Flores *et al.*, 1992; Lancis, 1998; Negri *et al.*, 1999; Negri & Villa, 2000; Raffi *et al.*, 2003; Wade & Bown, 2005; Lancis *et al.*, 2010) and is included in the CN9a subzone between the *D. berggrenii* and *A. primus* FO's. This increment was probably caused

by an ecological factor, given that these species predominate in the continental margins nannofloras assemblages (Haq, 1980). Flores *et al*. (1992) demonstrate that this was a synchronous event in some Mediterranean and north-Atlantic sections.

In the *Albatera* section the "small reticulofenestrids" are quite abundant throughout the section because the section was nearby the coast and nutrient-rich. The "small reticulofenestrids" flourish in such conditions, supporting the theory of high environmental stress (Aubry, 1992; Flores *et al*., 1995; Flores *et al*., 2005; Wade & Bown, 2005). The acme bottom cannot be precisely identified. However, from the bottom of the *Albatera* section and coinciding with the paracme of *R. pseudoumbilicus* the "small reticulofenestrids" become in general more abundant, with percentages as high as the 75% of the assemblage indicating that they are later than the acme beginning.

6.12 FO and FCO of *Discoaster surculus*

In general *D. surculus* (Figs 8-12) is scarce in the Mediterranean sections (Theodoridis, 1984; Raffi *et al*., 2003) but its presence has been established in the western Mediterranean basins (Martín-Pérez, 1997; Lancis, 1998; Lancis *et al*., 2010) in a good agreement with its biostratigraphic range in the equatorial Pacific (Gartner, 1992; Schneider, 1995; Lourens *et al*., 2004).

Discoaster surculus is scarce in our samples. Its first appearance is in the sample 15 of the *Albatera* section (Galería de los Suizos Marls), and the FCO was established in the sample 20, which was used as a secondary marker for the upper part of the CN9a/NN11a.

6.13 FO of the Initial *Amaurolithus* spp. (*Amaurolithus* cf. *primus*)

The *Amaurolithus* spp. FO (*A.* cf. *primus*) (Fig. 8-13; 8-14) represents an useful evolutionary event for worldwide biostratigraphic framework (Raffi *et al*., 1998). It marks the boundary between the subzones CN9a/CN9bA of Okada and Bukry (1980) emended by Raffi and Flores (1995), and NN11a/NN11b of Martini (1971). Some initial forms of *Amaurolithus* spp. (*A.* cf. *primus*) appear sporadically in the uppermost part of the *Albatera* section from sample 20 to the top of the section and coinciding with the FCO of *D. surculus*; thus, these forms are older than thought from previous observations.

6.14 FO of the *Syracosphaera pulchra*

Syracosphaera pulchra (Fig. 8-15) is present in the sediments from the Miocene until today. Despite the fragility and small size of this coccolith, it has been cited sporadically in the Miocene to Pliocene Mediterranean sections (Müller, 1978; Lancis, 1998). It should be pointed out that peak abundance was observed in the nearby Fortuna basin coinciding with the FCO of *D. surculus* (Lancis *et al*., 2010) and hence it would be considered a possible event to be evaluated in the future.

7. BIOSTRATIGRAPHIC CALIBRATION OF THE MAGNETOSTRATIGRAPHY DATA

7.1 Biostratigraphy

The Middle and Late Miocene index species in the Mediterranean do not always provide a robust biostratigraphic signal because they are scarce compared with the low-latitude oceans. However, we could recognize most of the events, as discussed in the previous section. The biohorizons of FO, FCO, LO and LCO identified in the composite *Les Moreres-Albatera* section provided a biozonal distribution pattern (Fig. 3) from the earliest to the latest Tortonian with a sedimentary gap marked by the Raya del Búho Conglomerates.

The bottom part of the *Les Moreres* section until the sample 23 can be assigned (Fig. 3) to the CN5b subzone (Okada & Bukry, 1980), equivalent to the NN7 of Martini (1971), by occurrence as the most significant species of the assemblage: *Discoaster kugleri, D. exilis, D. brouweri, D. aulakos, Helicosphaera walberdorfensis*, and *Coccolithus miopelagicus*. The FO of *Discoaster bellus* in sample 24, and the integrated forms *Discoaster micros/Catinaster coalitus* are considered to be the bottom of

the biozone CN6/NN8 (Okada & Bukry, 1980; Martini, 1971, respectively). Due to the scarcity of *Catinaster coalitus*, we have considered the subordinate FO events *D. bellus* and *D. micros/C. coalitus* to be sufficient to mark the base of the biozone (Lourens *et al.*, 2004; Raffi *et al.*, 2006). The first clear specimens of *Catinaster coalitus* appear in sample 26 and the first *D. hamatus* in the sample 31. The last FO marks the boundary between the biozone CN6/CN7 (Okada & Bukry, 1980) and NN8/NN9 (Martini, 1971). The upper part of the *Les Moreres* section show a uniform assemblage of the biozone CN7 (Okada & Bukry, 1980) and NN9 (Martini, 1971) by the presence of *Discoaster hamatus, D. bellus, D. micros, D. brouweri, D. variabilis, D. challengeri, D. bolli, D. neohamatus* (from the sample 44)*, D. calacaris* (sample 43)*, Catinaster coalitus, Reticulofenestra pseudoumbilicus, Coccolithus pelagicus, Calcidiscus macintyrei, C. leptoporus, Geminilithella rotula, Dictyococcites antarcticus, Triquetrorhabdulus rugosus,* and *Minylitha convallis* (sample 46).

The *Albatera* section should be included in the CN9a subzone (Okada & Bukry, 1980)/NN11a subzone (Martini, 1971) because of the presence of *Discoaster quinqueramus* and *D. berggrenii* marking the biozone CN9a (Okada & Bukry, 1980) and NN11A (Martini, 1971). Also the entire section is included in the PB of *R. pseudoumbilicus* > 7 µm, which register values of less than 5% throughout the section (Raffi *et al.*, 2003). On the other hand, this section is above the acme of the small reticulofenestrids included in the CN9a subzone between the *D. berggrenii* and *A. primus* FO's (Backman, 1978; Flores *et al.*, 1992; Lancis, 1998; Negri *et al.*, 1999; Negri & Villa, 2000; Raffi *et al.*, 2003; Wade & Bown, 2005; Lancis *et al.*, 2010).

The highest part of the section (sample 15) can be assigned to upper part of the CN9a/NN11a (Raffi *et al.*, 2003) by the presence of *D. surculus* (FCO in the sample 20) used as a secondary marker for the upper part of the CN9a/NN11a. The upper boundary between CN9a/CN9b is marked by the *A. primus* FO; however, the scarce initial forms assigned to *Amaurolithus* cf. *primus* that are found to be almost coincident with the FCO of *D. surculus* are forms prior to the FO of *Amaurolithus primus* str. s. These initial forms should be considered to be included in the CN9a, and also a more detailed study is needed to clarify the earliest evolution of the ceratoliths.

Palaeocologically, we should highlight the scarcity of asteroliths and the abundance of small reticulofenestrids such as *Lithostromathion perdurum*, *Pontosphaera multipora,* and different forms of *Scyphosphaera* spp. that could be related to a shallow and high-productivity environment (Martini, 1965; Bukry, 1976; Siesser, 1977; Gartner *et al.,* 1979; Flores, 1985; Chesptow-Lusty *et al.*, 1992; Raffi & Flores, 1995; Lancis, 1998; Flores *et al.*, 2005; Wade & Bown, 2006; Lancis *et al.*, 2010).

7.2 Magnetostratigraphy

The intensity of the NRM is relatively weak in the studied rocks ranging between 0.05 mA/m and 0.15 mA/m. Upon stepwise demagnetization two components can normally be distinguished in addition to a small viscous component removed at the first demagnetization step likely related to handling and/or storage. A low-field components conforming to the present geomagnetic field is removed up to fields of 17-21 mT. Then, a characteristic remanent magnetization (ChRM) is removed up to the maximum field applied (100 mT) that trends toward the origin of the diagram and presents dual polarity (Fig. 5B). We have established a ranking attending the quality of the demagnetization trajectories. Class A includes samples for which the ChRM component can be calculate unambiguously. Class B denotes samples with ambiguous ChRM components. The VPG latitude derived from the class A ChRM directions yields a succession of two magnetozones, characterized by reverse polarity in the lower part of the succession and reverse polarity in the upper part (Fig. 5A). The lowermost part of the studied succession of the Galeria de los Suizos Marls (interval 290-295 m) include two unreliable class B samples and only one normal class A sample and therefore this interval is reported as of ambiguous polarity and depicted in gray colour on the polarity column of Fig. 5A.

7.3 Calibration of the magnetostratigraphy with the new biostratigraphic data

For a comprehensive biomagnetostratigraphic correlation previous magnetostratigraphic results from the nearby *Rio*

Chicamo section (Dinarès-Turell *et al.*, 1999, and Krijgsman *et al.*, 2000) need to be taken into account. The *Rio Chicamo* section has recently been biostratigraphically calibrated with nannofossil data (Lancis *et al.*, 2010), supporting the magnetostratigraphic correlation A of Dinarès-Turell *et al.* (1999). The lowest magnetozone of the *Rio Chicamo* section was interpreted as a normal chron encompassing chrons C3Br.1n and C3Bn, therefore lacking expression of the intermediate short reverse chron C3Br.1r, because the FO of *Amaurolithus primus* is known to be located in chron C3Br.2r (Hilgen *et al.*, 2000; 7.341-7.170 Ma) just below chron C3Bn. Consequently, the top of the *Albatera* section is clearly below chron C3Br.2r of *Amaurolithus primus* FO.

The nannofossil data presented herein offers two different calibration points (Fig. 5). First, the FCO of *D. surculus* appears in other sections in chron C4n.2n, then the *Reticulophenestra pseudoumbilica* > 7 µm Paracme End occurs in the transition between C3Bn/C3Ar (Raffi *et al.*, 2006). Thus the *Albatera* section reverse and normal magnetozones shown in Figure 5 can be calibrated as chrons C4r.1r and C4n.2n respectively. Also the ambiguous polarity magnetozone and depicted in gray color on the polarity column of Fig. 5A can point to chron C4r.1n but better samples are needed to confirm this.

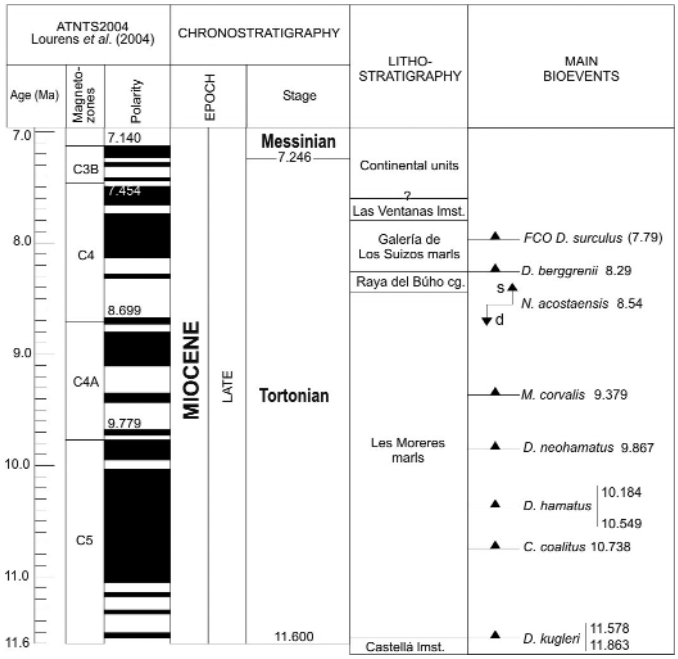

Figure 13. Summary of the positions of the biohorizons in the time interval 11.6 -7.8 Ma, relative to planktonic foraminifera and calcareous nannoplankton.

8. DISCUSSION AND CONCLUSIONS

The sedimentation over the structured basement of the Crevillente Sierra started with the El Castellà limestone. As this unit has not been sampled, no direct dating is possible, but in the previous work of Tent-Manclús *et al.* (2004) some marly intervals are dated in a nearby section as Serravallian by the presence of *Discoaster heteromorphus* plus *D. kugleri*.

Then the sedimentation shifts to the Les Moreres Marls lithological unit, which yields abundant planktonic foraminifera and calcareous nannofossils. The lowest portion of the unit indicates by its microfossil content an interval near the Serravallian-Tortonian boundary (Fig. 13). The absence of planktonic foraminifera *Globigerinoides subquadratus* points to a Tortonian age but the presence of *D. kugleri* indicates the interval between the Serravallian-Tortonian boundary, and, depending on whether it is considered above or below the LCO, it could be assigned to the Tortonian or Serravallian, respectively. Thus the bottom part of the Les Moreres Marls is considered to be earliest Tortonian without ruling out a latest Serravallian age. The planktonic foraminifera and the calcareous nannofossils (Fig. 13) do not show any time gap from the bottom of the section assigned to the MMi9 planktonic foraminifera biozone (Lourens *et al.*, 2004) and CN5b/NN7 calcareous nannoplankton biozones (Okada & Bukry, 1980; Martini, 1971) to the to MMi11 planktonic foraminifera biozone (Lourens *et al.*, 2004) CN7/NN9 (Okada & Bukry, 1980; Martini, 1991). The top of the Les Moreres Marls can be calibrated by the dextral to sinistral change in *Neogloboquadina acostaensis* estimated at 9.54 Ma by Lourens *et al.* (2004).

The Raya del Búho Conglomerate gradually overlie the Les Moreres Marls but the upper contact had developed an encrusted level interpreted as a possible time gap. This unit should be included in the MMi11 planktonic foraminifera biozone (Lourens *et al.*, 2004) and CN7/NN9 calcareous nannoplankton biozones (Okada & Bukry, 1980; Martini, 1971).

The bottom part of the Galería de los Suizos Marls in the *Albatera* section show a planktonic foraminifera assemblage included in the MMi12a biozone, and thus the foraminifera biozones do not have sufficient resolution to measure the time gap. However, the calcareous nannofossil assemblage with the FOs of *D. neorectus* and *D. quinqueramus* indicate the CN9a/NN11a biozones (Okada & Bukry, 1980; Martini, 1971) and can be calibrated by the FO of *D. berggrenii* as 8.29 Ma (Lourens *et al*., 2004). The time gap between the Raya del Búho Conglomerate and the Galería de los Suizos Marls could be estimated at about 1.2 Ma. This discontinuity was caused by a NW-SE faulting tectonic event (Tent-Manclús, 2003). The Galería de los Suizos Marls fossilized those faults.

The *Albatera* section yields palaeomagnetic data shown in Figure 5 that can be calibrated as chrons C4r.1r and C4n.2n. The transition between those chrons was calibrated by Lourens *et al*. (2004) at 8.108 Ma. The top of the section is above the *D. surculus* FCO, calibrated at 7.79 Ma (Lourens *et al*., 2004) which allows us to calibrate the bottom of the overlying Las Ventanas Limestones as younger than that age.

The composite *Les Moreres-Albatera* section should be considered as the most complete Tortonian section of the Betic Cordillera.

9. ACKNOWLEDGEMENTS

This work has been supported by the projects CGL2007-65832/BTE, PASUR CGL2009-08651 MCI, and CGL2009-07830 MCI, and the research group VIGROB-167. CL was funded by the research grant BEST/2010/068 GVA. We are indebted to David Nesbitt for correcting the English version of the paper.

10. REFERENCES

Alfaro García, P. 1995. *Neotectónica en la Cuenca del Bajo Segura (Extremo oriental de la Cordillera Bética).* Ph. D. Thesis Univ. Alicante, Spain. 219 pp. (unpublished). http://hdl.handle.net/10045/3176

Aubry, M. P. 1992. Late paleogene calcareous nannoplankton evolution: a tale of climatic deterioration. In: *Eocene-Oligocene Climatic and Biotic Evolution* (Eds. D. R. Prothero and W. A. Berggren, W. A.). Princeton University Press, 272-309.

Azéma, J. and Montenat, C. 1975. *Mapa y memoria explicativa de la Hoja 892 (Fortuna) del Mapa Geológico Nacional a escala 1:50.000*. I.G.M.E., Madrid.

Backman, J. 1978. Late Miocene-Early Pliocene nannofossil biochronology and biogeography in the Vera basin, S.E. Spain. *Act. Univ. Stock. Contrib. Geol.*, 32, 2, 93-114.

Backman, J., Pestiaux, P., Zimmerman, H. and Hermelin, O. 1986. Paleoclimatic and Paleogeographic development in the Pliocene North Atlantic: *Discoaster* accumulation and coarse fraction data. In: North Atlantic Paleoceanography (Eds. C. P. Summerhayes and N. J. Shackleton). *Geological Society Special Publication*, 21, 231-242.

Backman, J. and Raffi, I. 1997. Calibration of Miocene nannofossil events to orbitally-tuned cyclostratigraphies from Ceara Rise. In: (Eds. N. J. Shackleton, W. B. Curry, C. Richter, and T. J. Bralower), Proceeding ODP, Scientific Results, 154, 83-99. doi: 10.2973/odp.proc.sr.154.101.1997

Bukry, D. 1971. Cenozoic calcareous nannofossils from the Pacific Ocean. *Transactions of the San Diego Society of Natural History,* 16, 4, 303-328.

Bukry, D. 1973. Low-Latitude coccolith biostratigraphic zonation. In: (Eds. N. T. Edgar, J. B. Saunders, *et al.*), Init. Repts. DSDP 15, (U.S. Govt. Print. Off.), 685-703. doi: 10.2973/dsdp.proc.15.116.1973

Bukry, D. 1976. Coccolith stratigraphy of Manihiki Plateau, Central Pacific, Deep Sea Drilling Project, site 317. In: (Eds. S. O. Schlanger, E. D. Jackson, *et al.*), Init. Repts. DSDP 33, Washington (U. S. Govt. Print Off.), 493-499. doi: 10.2973/dsdp.proc.33.115.1976

Bukry, D. 1981. Cenozoic Coccoliths from the Deep Sea Drilling Project. *SEPM special publication*, 32, 335.

Bukry, D. and Percival, S. E. 1971. New Tertiary calcareous nannofossils. *Tulane Studies in Geology and Paleontology*, 8, 123-146.

Caruso, A., Sprovieri, M., Bonanno, A. and Sprovieri, R. 2002. Astronomical calibration of the Serravallian-Tortonian Case Pelacani section (Sicily, Italy). In: Integrated Stratigraphy and Paleoceanography of the Mediterranean Middle Miocene (Ed. S. Iaccarino). *Riv. Ital. Paleontol. Stratigr.,* 108, 297-306.

Chesptow-Lusty, A., Shackleton, N.J. and Backman, J. 1992. Upper Pliocene *Discoaster* abundance from the Atlantic, Pacific, and Indian oceans: the significance of productivity pressure at low latitudes. *Mem. Sci. Geol.*, 44, 357-373.

Dinarès-Turell, J., Ortí, F., Playà, E. and Rossell, L. 1999. Palaeomagnetic chronology of the evaponritic sedimentation in the Neogene Fortuna Basin (SE Spain): early restriction preceding the 'Messinian Salinity Crisis'. *Palaeogeography, Palaeoclimatology, Palaeoecology,* 154, 161-178.

Flores, J. A. 1985. *Nanoplancton calcáreo en el Neógeno del borde noroccidental de la Cuenca del Guadalquivir (S.O. de España).* Ph. D. Thesis, Univ. Salamanca, Spain.

Flores, J. A. and Sierro, F. J. 1987. Calcareous plankton in the Tortonian-Messinian transition of the Northwestern edge of the Guadalquivir Basin (SW Spain). *Abhandlunden der Geologischen Bundesanstalt*, 39, 64-87.

Flores, J. A. and Sierro, F. J. 1989. Calcareous nannoflora and planktonic foraminifera in the Tortonia/Messinian boundary interval of East At-

lantic DSDP sites and their relation to Spanish and Moroccan sections. In: *Nannofossils and their applications* (Eds. S. Van Heck, and J. Crux). London: Ellis Horwood, 249-266.

Flores, J. A., Sierro, F. J. and Glaçon, G. 1992. Calcareous plankton analysis in the pre-evaporitic sediments of the ODP site 654 (Tyrrhenian sea, Western Mediterranean). *Micropaleontology*, 38, 3, 279-288.

Flores, J. A., Sierro, F. J. and Raffi, I. 1995. Evolution of the calcareous nannofossil assemblage as a response to the paleoceanographic changes in the eastern equatorial Pacific Ocean from 4 to 2 Ma (Leg 138, Sites 849 and 852). In: (Eds. N. G. Pisias, L. A. Mayer, T. R. Janecek, A. Palmer-Julson and T. H. van Andel). Proceedings ODP, Scientific Results 138, 163– 176. doi: 10.2973/odp.proc.sr.138.108.1995

Flores, J. A., Sierro F. J., Gabriel M. Filippelli G. M., Bárcena M. A., Pérez-Folgado M., Vázquez A. and Utrilla, R. 2005. Surface water dynamics and phytoplankton communities during deposition of cyclic late Messinian sapropel sequences in the western Mediterranean. *Marine Micropaleontology*, 56, 50–79.

Fornaciari, E., Raffi, I., Rio, D., Villa, G., Backman, J. and Olafsson, G. 1990. Quantitative distribution patterns of Oligocene and Miocene calcareous nannofossils from the western equatorial Indian Ocean. In: (R. A. Duncan, J. Backman, L. C. Peterson *et al.*) Proceedings ODP, Sci. Results 115, 237-254.

Fornaciari, E., Di Stefano, A. Rio, D. and Negri, A. 1996. Middle Miocene quantitative calcareous nannofossil bioestratigraphy in the Mediterranean region. *Micropaleontology*, 42, 1, 37-63.

Foresi, L.M., Bonomo, S., Caruso, A., Di Stefano, A., Di Stefano, E., Iaccarino, S.M., Lirer, F., Salvatorini, G. and Sprovieri, R. 2002. High-resolution calcareous plankton biostratigraphy of the serravallian succession of the Tremiti Islands (Adriatic Sea, Italy). In: Iaccarino, S. (Ed.), Integrated Stratigraphy and Paleoceanography of the Mediterranean Middle Miocene. *Rivista Italiana di Paleontolologia e Stratigrafia*, 108, 257-273.

Gartner, S. 1992. Miocene nannofossil chronology in the North Atlantic DSDP Site 608. *Marine Micropaleontology,* 18, 307-331.

Gartner, S. and Bukry, D. 1975. Morphology and phylogeny of the Coccolithophycean family Ceratolithaceae. Journal Research. U. S. Geological Survey 3, 4, 451-465.

Gartner, S., Chen, M. P. and Stanton, R. J. 1979. Late Neogene history in the American Mediterranean. VII Int. Cong. Med. Neog. Athens. *Annales Géologiques des Pays Helléniques*, Tome Hors série, 1, 425-437.

Groupe de Recherche Néotectonique de l'arc de Gibraltar (1977): L'histoire tectonique récente (Tortonien à Quaternaire) de l'Arc de Gibraltar et des bordures de la mer d'Alboran. *Bulletin Société Géologique de France*, 19, 575-614.

Hilgen, F. J., Krijgsman, W., Langereis, C. G., Lourens, L. J., Santerelli, A. and Zachariasse, W. J. 1995. Extending the astronomical (polarity) time scale into the Miocene. *Earth Planetary Science Letters*, 136, 495– 510.

Hilgen, F.J., Krijgsman, W., Raffi, I., Turco, E. and Zachariasse, W. J. 2000. Integrated stratigraphy and astronomical calibration of the Serravallian/Tortonian boundary section at Monte Gibliscemi (Sicily, Italy). *Marine Micropaleontology*, 38, 182-211.

Hilgen, F. J., Abdul Aziz, H., Krijgsman, W., Raffi, I. and Turco, E. 2003. Integrated stratigraphy and astronomical tuning of the Serravallian and lower Tortonian at Monte dei Corvi (Middle-Upper Miocene, northern Italy). *Palaeogeography, Palaeoclimatology, Palaeoecology*, 199, 229-264.

Kirschvink, J. L. 1980. The least-square line and plane and analysis of paleomagnetic data. *Geophysical Journal of the Royal Astronomical Society*, 62, 699-718.

Krijgsman, W., Garcés, M., Agustí, J., Raffi, I., Taberner, C. and Zachariasse, W. J. 2000. The 'Tortonian salinity crisis' of the eastern Betics (Spain). *Earth and Planetary Science Letters*, 181, 497-511.

Lancis, C. 1998. *El nanoplancton calcáreo de las cuencas neógenas orientales de la Cordillera Bética.* Ph.D. Thesis, Univ. Alicante, Spain, 841 pp. http://hdl.handle.net/10045/7944

Lancis, C., Tent-Manclús, J.E., Soria, J. M., Caracuel, J. E., Corbí, H., Dinarès-Turell, J., Estévez, A. and Yébenes, A. 2010. Nannoplankton biostratigrphic calibration of the evaporitic events in the Neogene Fortuna Basin (SE Spain). *Geobios,* 43, 201-217. doi: 10.1016/j.geobios.2009.09.007

Lourens, L., Hilgen, F., Shackleton, N. J., Laskar, J. and Wilson, D. 2004. The neogene period. In: *A geologic Time Scale* (Eds. F. M. Gradstein, J. G. Ogg and A. G. Smith). Cambridge University Press, 409-440.

Mazzei, R., 1985. The Miocene sequence of the Maltese islands: biostratigraphic and chronostratigraphic reference based on nannofossils. *Atti della Società Toscana di Scienze Naturali*, Serie A, 92, 165-197.

Martín-Pérez, J. A. 1997. *Nanoplancton calcáreo del Mioceno de la Cordillera Bética (Sector Oriental).* Ph. D. Thesis, Univ. Granada, Spain, 329 pp. (unpublished)

Martini, E. 1965. Mid-Tertiary calcareous nannoplankton from Pacific deep-sea cores. In: *Submarine Geology and Geophysics* (Eds. W. F. Whittard and R. B. Bradshaw). Proc. 17th Symp. Colston Res. Soc. London, 393-411.

Martini, E. 1971. Standard Terciary and Quaternary calcareous nannoplankton zonation. Proc. II Planktonic conference, Tecnoscienza, Roma, 2, 736-785.

Mazzei, R. 1985. The Miocene sequence of the Maltese islands: biostratigraphic and chronostratigraphic references based on nannofossils. *Atti della Società Toscana di Scienze Natural, Memorie*, 42, 165-197

Montenat, C. 1977. *Les bassins néogènes du levant d'Alicante et de Murcia (Cordillères bétiques orientales-Espagne). Stratigraphie, paléogéographie et évolution dynamique.* Documents Laboratoire Géologie Faculté des Sciences de Lyon, 69, 345 pp.

Montenat, C., Ott d'Estevou, Ph. and Coppier, G. 1990. Les basins neogenes entre Alicante et Cartagena. In: *Les Bassins Néogènes du Domaine Bétique Orientale (Espagne)* (Ed. C. Montenat). Documents et Travaux, Institut Géologique Albert de Lapparent, 12-13, 313-368.

Müller, C. 1978. Neogene calcareous nannofossils from the Mediterranean - Leg 42A of the Deep Sea Drilling Project. In: (Eds. K. J. Hsü, L. Montadert *et al.*). *Initial Reports DSDP*, 42 (Pt. 1), 727-751.

Müller, C. 1990. Nannoplankton biostratigraphy and paleoenvironmental interpretations from the Tyrrhenian Sea, ODP Leg 107 (Western

Mediterranean). In: Kastens, K. A., Mascle, J. *et al*., (Eds.), Proceedings ODP, Scientific Results, 107, 495-511.

Negri, A., Giunta, S., Hilgen, F., Krijgsman, W. and Vai, G. B. 1999. Calcareous nannofossil biostratigraphy of the M. del Casino section (northern Apennines, Italy) and paleoceanographic conditions at times of Late Miocene sapropel formation. *Marine Micropaleontology*, 36, 1, 13-30.

Negri, A. and Villa, G. 2000. Calcareous nannofossil biostratigraphy biochronology and paleoecology at the Tortonian/Messinan boundary of the Faneromeni section (Crete). *Palaeogeography, Palaeoclimatology, Palaeoecology,* 156, 195-209.

Okada, H. and Bukry, D. 1980. Supplementary modification and introduction of code numbers to the low-latitude coccolith biostratigraphic zonation (Bukry, 1973; 1975). *Marine Micropaleontology*, 5, 321-325.

Raffi, I. and Flores, J.A. 1995. Pleistocene through Miocene Calcareous nannofossils from eastern equatorial Pacific Ocean (Leg 138). In: (Eds. N. G. Pisias, L. A. Mayer, T. R. Janecek, A. Palmer-Julson and T. H. van Andel). Proceedings ODP, Scientific Results 138, 233-285. doi: 10.2973/odp.proc.sr.138.112.1995

Raffi, I., Backman, J. and Rio, D. 1998. Evolutionary trends of calcareaous nannofossils in the Late Neogene. *Marine Micropaleontology*, 35, 17-41.

Raffi, I., Backman, J., Fornaciari, E., Pälike, H., Rio, D., Lourens, L. and Hilgen, F. 2006. A review of calcareous nannofossil astrobiochronology encompassing the past 25 million years. *Quaternary Science Reviews*, 25, 3113-3137. doi:10.1016/j.quascirev.2006.07.007

Raffi, I., Mozzato, C., Fornaciari, E., Hilgen, F. J. and Rio, D. 2003. Late Miocene calcareaous nannofossil biostratigraphy and astrobiochronology for the Mediterranean region. *Micropaleontology*, 49 (1), 1-26. doi:10.2113/49.1.1

Raffi, I., Rio, D., d'Afri, A., Fornaciari, E. and Rochetti, S. 1995. Quantitative distribution patterns and biomagnetostratigraphy of Middle and Late Miocene calcareous nannofossils from equatorial Indian and Pacific Ocean (legs 115, 130 and 138). In: (Eds. N. G. Pisias, L. A. Mayer, T. R. Janecek, A. Palmer-Julson and T. H. van Andel). Proceedings ODP, Scientific Results, 138, 479-502. doi: 10.2973/odp.proc.sr.138.125.1995

Rio, D., Mazzei, R. and Palmieri, G. 1976. The stratigraphic position of the Mediterranean Upper Miocene evaporites, based on nannofossils. *Memorie della Societá Geoligica Italiana,* 16, 261-276

Rio, D., Fornaciari, E. and Raffi, I. 1990. Late Oligocene through early Pleistocene calcareous nannofossils from western equatorial Indian Ocean (Leg 115). In: (Eds. R. A. Duncan, J. Backman, L. C. Peterson, *et al*.). Proceedings ODP, Scientific Results, 115, 175-235. doi: 10.2973/odp.proc.sr.115.152.1990

Rodríguez-Fernández, J., Comas, M. C., Soria, J., Martín-Pérez, J. A. and Soto, J. I. 1999. The Sedimentary record of the Alboran basin: an attempt at sedimentary sequence correlation and subsidence analysis. In: (Eds. R. Zahn, M. C. Comas and A. Klaus). Proceedings ODP, Scientific Results, 161, 69-76. doi:10.2973/odp.proc.sr.161.207.1999

Santisteban Bové, C. 1981. *Petrología y sedimentología de los materiales del Mioceno superior de la cuenca de Fortuna (Murcia), a la luz de la crisis de salinidad.* Ph.D. Thesis, Univ. Barcelona, Spain. (unpublished)

Schneider, D. A. 1995 Paleomagnetism of some ODP Leg 138 sediments: detailing Miocene magnetostatigraphy. In: (Eds. N. G. Pisias, L. A. Mayer, T. R. Janecek, A. Palmer-Julson and T. H. van Andel). Proceedings ODP, Scientific Results, 138, 59-72. doi: 10.2973/odp.proc.sr.138.105.1995

Shackleton, N. J. and Crowhurst, S. 1997. Sediment fluxes based on an orbitally tuned time scale 5 Ma to 14 Ma, Site 926. In: (Eds. N. J. Shackleton, W. B. Curry, C. Richter and T. J. Bralower). Proceeding ODP, Scientific Results, 154, 69-82. doi:10.2973/odp.proc.sr.154.102.1997

Siesser, W. G. 1997. Calcareous nannofossils as age and paleoenvironmental indicators. Electron van. Sudelike Afrika. In: Proc., 7. Elec. Micros. Soc. South Africa., 81-82.

Soria, J. M., Alfaro, P., Fernández, J. and Viseras, C. 2001. Quantitative subsidence-uplift analysis of the Bajo Segura Basin (eastern Betic Cordillera, Spain): tectonic control on the stratigraphic architecture. *Sedimentary Geology*, 140, 271-289.

Soria, J.M., Fernández, J. and Viseras, C. 1999. Late Miocene stratigraphic evolution of the intramontane Guadix Basin (Central Betic Cordillera, Spain): implications for an Atlantic-Mediterranean connection. *Palaeogeography, Palaeoclimatology, Palaeoecology*, 151, 255-266.

Soria, J. M., Fernández, J., García, F. and Viseras, C. 2003. Correlative lowstand deltaic and shelf systems in the Guadix Basin (Late Miocene, Betic Cordillera, Spain): The stratigraphic record of forced and normal regressions. *Journal of Sedimentary Research*, 73, 6, 912-925. doi:1527-1404/03/073-912.

Soria, J. M., Tent-Manclús, J. E., Caracuel, J. E., Yébenes, A., Lancis, A. and Estévez, A. 2005. La crisis de salinidad Tortoniense: su registro en la zona de enlace entre las cuencas de Fortuna y del Bajo Segura. *Geo-Temas,* 8, 113-118.

Tent-Manclús, J. E. 2003. *Estructura y estratigrafía de las sierras de Crevillente, Abanilla y Algayat: su relación con la Falla de Crevillente.* Ph.D. Thesis, Univ. Alicante, Spain, 957 pp. http://hdl.handle.net/10045/10414

Tent-Manclús, J. E., Yébenes, A. and Estévez, A. 2005. ¿Por qué son tan diferentes las sierras de Crevillente y Abanilla? *Geogaceta*, 37, 71-74

Tent-Manclús, J. E., Lancis, C., Soria, J. M., Dinarès-Turell, J., Estévez, A., Caracuel, J. E. and Yébenes, A. 2007. Primeros datos bioestratigráficos de los grupos evaporíticos de la Cuenca de Fortuna (Cordillera Bética). *Geogaceta*, 41, 231-234.

Tent-Manclús, J. E., Lancis, C., Yébenes, A. and Estévez, A. 2004. Estratigrafía del Mioceno Medio y Superior al NW de Crevillente (Alicante). *Geo-Temas*, 7, 185-190.

Tent-Manclús, J. E., Soria, J. M., Estévez, A., Lancis, C., Caracuel, J. E., Dinarès-Turell, J. and Yébenes, A. 2008. Tortonian Salinity Crisis and tectonics: A view from the Fortuna Basin (SE Spain). *Comptes Rendus Geoscience,* 340, 474-481. doi: 10.1016/j.crte.2008.05.003

Theodoridis, S. A. 1984. Calcareous nannofossils biozonation of the Miocene and revision of the Helicoliths and Discoasters. *Utrecht Micropaleontological Bulletin,* 31, 271 pp.

Viseras, C., Soria, J. M. and Fernández, J. 2004. Cuencas neógenas postorogénicas de la Cordillera Bética. In: *Geología de España* (Ed. J. A. Vera). SGE-IGME, Madrid, 576-581.

Vera, J. A. (Ed.) 2004. Cordillera Bética y Baleares. In: *Geología de España* (Ed. J. A. Vera). SGE-IGME, Madrid, 345-464.

Wade, B. S. and Bown, P. R. 2006. Calcareous nannofossils in extreme environments: The Messinian Salinity Crisis, Polemi Basin, Cyprus. *Palaeogeography, Palaeoclimatology, Palaeoecology*, 233, 271-286. doi:10.1016/j.palaeo.2005.10.007

Zijderveld, J. D. A. 1967. A.C. demagnetization of rock: analysis of results. In: *Methods in paleomagnetism* (Eds. D. W. Collinson, K. M. Creer, S. K. Runcorn). Elsevier, Amsterdam, 254-286.

Manuscrito Recibido: 18 de mayo, 2010
Manuscrito Aceptado: 28 de noviembre, 2010

Appendix A

Taxonomic list of the calcareous nannoplankton considered in this work (see Young, 1998)

Amaurolithus primus (Bukry & Percival, 1971) Gartner & Bukry, 1975
Calcidiscus macintyrei (Bukry & Bramlette, 1969) Loeblich & Tappan, 1968
C. leptoporus (Murray & Blackman, 1898) Loeblich & Tappan, 1978
Coccolithus pelagicus (Wallich, 1871) Schiller, 1930
C. miopelagicus Bukry, 1971
Catinaster coalitus Martini & Bramlette, 1963
Dictyococcites antarcticus Haq, 1976 = *Reticulofenestra antarctica* Haq, 1976
D. productus (Kamptner, 1963) emend. Backman, 1980
Discoaster aulakos Gartner, 1967
D. bellus Bukry & Percival, 1971
D. berggrenii Bukry, 1971
D. bolli Martíni & Bramlette, 1963
D. brouweri Tan Sin Hok, 1927 emend. Bramlette & Riedel, 1954
D. calcaris Gartner, 1967
D. challengeri Bramlette & Riedel, 1954
D. exilis Martini & Bramlette, 1963
D. hamatus Martini & Bramlette, 1963
D. intercalaris Bukry, 1971
D. loeblichii Bukry, 1971
D. kugleri Martini & Bramlette, 1963
D. micros Theodoridis, 1984
D. neohamatus Bukry & Bramlette, 1969
D. neorectus Bukry, 1971
D. pentaradiatus Tan Sin Hok, 1927 emend. Bramlette & Riedel, 1954
D. prepentaradiatus Bukry & Percival, 1971
D. pseudovariabilis Martini & Worsley, 1971
D. quinqueramus Gartner, 1969
D. surculus Martini & Bramlette, 1963
D. tamalis Kamptner, 1967
D. triradiatus Tan, 1927
D. variabilis Martini & Bramlette, 1963
Geminilithella jafarii (Müller, 1974) Backman, 1980
G. rotula (Kamptner, 1948) Backman, 1980
Helicosphaera carteri (Wallich, 1877) Kamptner, 1954
H. rhomba Bukry, 1971
H. stalis Theodoridis, 1984
H. walberdorsfensis Müller, 1974
Lithostromation perdurum Deflandre, 1942
Pontosphaera multipora (Kamptner, 1948) Roth, 1970
Reticulofenestra gelida (Geitzenauer, 1972) Backman, 1978
R. haqii Backman, 1978
R. minuta (Roth, 1970)
R. minutula Gartner, 1967
R. pseudoumbilicus (Gartner, 1967) Gartner, 1969
Scyphosphaera amphora Deflandre, 1942
Scy. conica Kamptner, 1955
Scy. apsteinii Lohmann, 1902
Scy. intermedia Deflandre, 1942
Sphenolithus abies Deflandre *in* Deflandre & Fert, 1954
Sph. neoabies Bukry & Bramlette, 1969
Sph. moriformis (Brönnimann & Stradner, 1960) Bramlette & Wilcoxon, 1967
Syracosphaera pulchra Lohmann, 1902
Triquetrorhabdulus rugosus Bramlette & Wilcoxon, 1967
Small reticulofenestrids (nannolith size smaller than 3 m, independently of central area properties: *Dictyococcites productus* (Kamptner, 1963) emend. Backman, 1980 plus *Reticulofenestra minuta* Roth, 1970)